18. Micro/Nanorobots

Bradley J. Nelson, Lixin Dong, Fumihito Arai

The field of microrobotics covers the robotic manipulation of objects with dimensions in the millimeter to micron range as well as the design and fabrication of autonomous robotic agents that fall within this size range. Nanorobotics is defined in the same way only for dimensions smaller than a micron. With the ability to position and orient objects with micron- and nanometer-scale dimensions, manipulation at each of these scales is a promising way to enable the assembly of micro- and nanosystems, including micro- and nanorobots.

This chapter overviews the state of the art of both micro- and nanorobotics, outlines scaling effects, actuation, and sensing and fabrication at these scales, and focuses on micro- and nanorobotic manipulation systems and their application in microassembly, biotechnology, and the construction and characterization of micro and nanoelectromechanical systems (MEMS/NEMS). Material science, biotechnology, and micro- and nanoelectronics will also benefit from advances in these areas of robotics.

18.1 Overview of Micro- and Nanorobotics

Progress in robotics over recent years has dramatically extended our ability to explore, perceive, understand, and manipulate the world on a variety of scales extending from the edges of the solar system, to the bottom of the sea, down to individual atoms (Fig. 18.1). At the lower end of this scale, technology has been moving toward greater control of the structure of matter, suggesting the feasibility of achieving thorough control of the molecular structure of matter atom by atom, as Richard Feynman first proposed in 1959 in his prophetic article on miniaturization [18.1]:

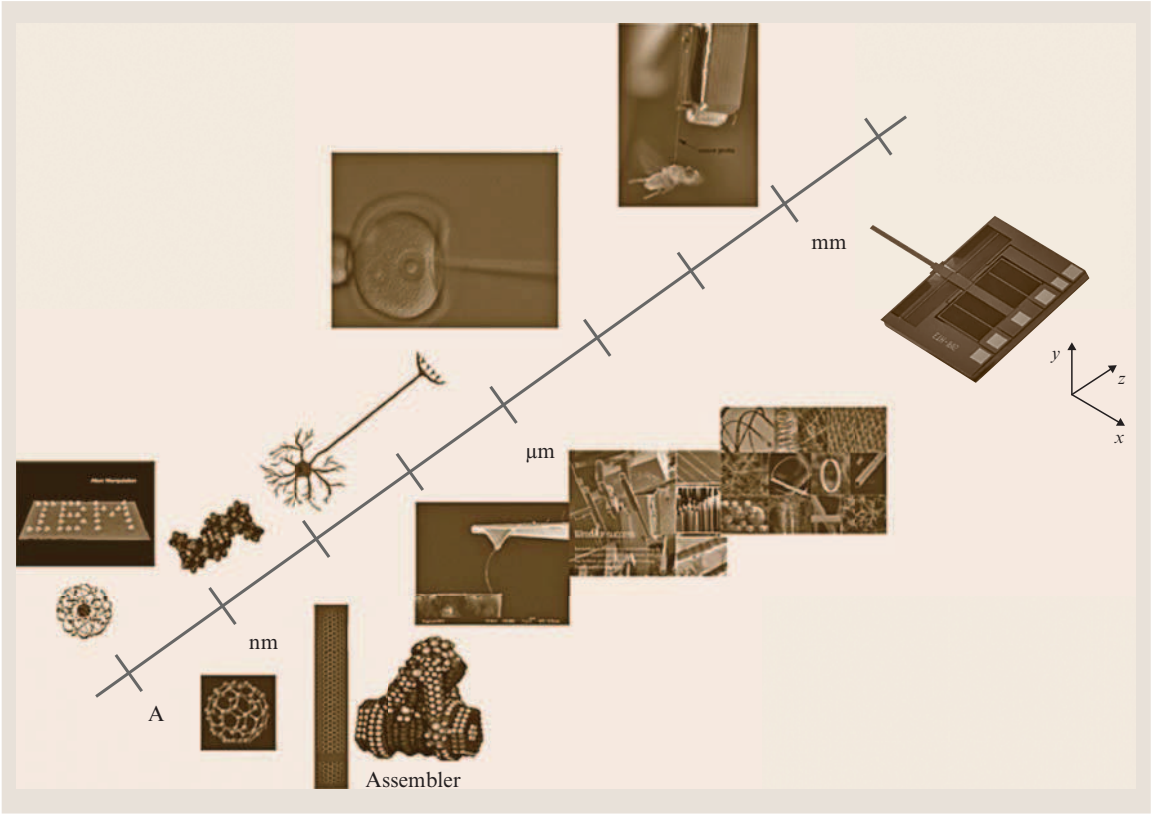

Fig. 18.1 Robotic exploration at micro- and nanometer scales

> *What I want to talk about is the problem of manipulating and controlling things on a small scale . . . I am not afraid to consider the final question as to whether, ultimately – in the great future – we can arrange the atoms the way we want: the very atoms, all the way down!*

He asserted that

> *At the atomic level, we have new kinds of forces and new kinds of possibilities, new kinds of effects. The problems of manufacture and reproduction of materials will be quite different. The principles of physics, as far as I can see, do not speak against the possibility of maneuvering things atom by atom.*

This technology is now labeled *nanotechnology*.

The *great future* of Feynman began to be realized in the 1980s. Some of the capabilities he dreamed of have been demonstrated, while others are being actively pursued. Feynman foresaw the possibility of employing a microrobotic manipulator (*a master–slave system*) for bottom-up manufacturing (manipulation, assembly, etc.) of minute machines; one such device he described as "swallowing the surgeon", which he attributed to his friend Albert R. Hibbs. He also imagined we could "build a billion tiny factories, models of each other, which are manufacturing simultaneously, drilling holes, stamping parts, and so on." Micro- and nanorobotics research has progressed from these seemingly *far-out* concepts of the 1960s and 1970s to reality when microelectromechanical systems (MEMS) began to emerge in the late 1980s. These building blocks took the form of surface-micromachined micromotors and microgrippers made of polysilicon fabricated on a silicon chip [18.2]. In the late 1980s and early 1990s, more concrete suggestions on how one could realize MEMS-based microrobotic devices using such micromotors as well as potential applications were published [18.3, 4]. Today, a variety of microrobotic devices are enabling new applications in various fields.

In industry, interesting areas for microrobotics include assembly [18.5, 6], characterization, inspection and maintenance [18.7, 8], microoptics (positioning of microoptical chips, microlenses and prisms) [18.9], and microfactories [18.10]. Many of these applications require automated handling and assembly of small parts with accuracy in the submicron range.

Other important fields include biology (manipulation, capturing, sorting and combining cells [18.11]) and medical technology [18.12, 13]. In surgery, the use of steerable catheters and endoscopes is very attractive and the development of increasingly small microrobotic devices is rapidly progressing. Wireless untethered microrobots that will explore and repair our bodies ("swallowing the surgeon") appear to be simply a matter of time. In fact, endoscopy using wireless capsules (camera pills) are already on the market and allow for endoscopic imaging of the entire gastrointestinal tract [18.14], something currently not possible using standard scopes. Magnetic steering or crawling-type motions serve as promising ways for such devices to locomote in a controlled fashion [18.15]. Doctors could steer pill-mounted cameras and other actuators to areas of interest for visual investigation and biopsies beyond the range of current endoscopes.

Nanorobotics represents the next stage in miniaturization for maneuvering nanoscale objects. Nanorobotics is the study of robotics at the nanometer scale, and includes robots that are nanoscale in size, i. e., nanorobots, and large robots capable of manipulating objects that have nanometer dimensions with nanometer resolution, i. e., nanorobotic manipulators. The field of nanorobotics brings together several disciplines, including nanofabrication processes used for producing nanoscale robots, nanoactuators, nanosensors, and physical modeling at nanoscales. Nanorobotic manipulation technologies, including the assembly of nanometer-sized parts, the manipulation of biological cells or molecules, and the types of robots used to perform these types of tasks also form a component of nanorobotics.

As the 21st century unfolds, the impact of nanotechnology on the health, wealth, and security of humankind is expected to be at least as significant as the combined influences in the 20th century of antibiotics, the integrated circuit, and human-made polymers. For example, N. Lane stated in 1998, "If I were asked for an area of science and engineering that will most likely produce the breakthroughs of tomorrow, I would point to nanoscale science and engineering." [18.16] The great scientific and technological opportunities nanotechnology presents have stimulated extensive exploration of the nanoworld and initiated an exciting worldwide competition, which has been accelerated by the publication of the *National Nanotechnology Initiative* by the US government in 2000 [18.17]. Nanorobotics will play a significant role as an enabling nanotechnology and could ultimately be a core part of nanotechnology if Drexler's machine-phase nanosystems based on self-replicative molecular assemblers via mechanosynthesis can be realized [18.18].

By the early 1980s, scanning tunneling microscopes (STMs) [18.19] radically changed the way in which we interacted with and even regarded single atoms and molecules. The very nature of proximal probe methods encourages the exploration of the nanoworld beyond conventional microscopic imaging. Scanning probes now allow us to perform *engineering* operations on single molecules, atoms, and bonds, thereby providing a tool that operates at the ultimate limits of fabrication. They have also enabled exploration of molecular properties on an individual nonstatistical basis.

STMs and other nanomanipulators are nonmolecular machines that use bottom-up strategies. Although performing only one molecular reaction at a time is obviously impractical for making large amounts of a product, it is a promising way to provide the next generation of nanomanipulators. Most important, it is possible to realize the directed assembly of molecules or supermolecules to build larger nanostructures through nanomanipulation. The products produced by nanomanipulation could be the first step of a bottom-up strategy in which these assembled products are used to self-assemble into nanomachines.

One of the most important applications of nanorobotic manipulation will be nanorobotic assembly. However, it appears that, until assemblers capable of replication can be built, the combination of chemical synthesis and self-assembly are necessary when starting from atoms; groups of molecules can self-assemble quickly due to their thermal motion, enabling them to *explore* their environments and find (and bind to) complementary molecules. Given their key role in natural molecular machines, proteins are obvious candidates for early work in self-assembling artificial molecular systems. *Degrado* [18.20] demonstrated the feasibility of designing protein chains that predictably fold into solid molecular objects. Progress is also being made in artificial enzymes and other relatively small molecules that perform functions like those of natural proteins. Several bottom-up strategies using self-assembly appear feasible [18.21]. Chemical synthesis, self-assembly, and

supramolecular chemistry make it possible to provide building blocks at relatively large sizes beginning from the nanometer scale. Nanorobotic manipulation serves as the base for a hybrid approach to construct nanodevices by structuring these materials to obtain building blocks and assembling them into more complex systems.

Despite the claims of many *futurists*, the form nanorobots of the future will take and what tasks they will actually perform remain unclear. However, it is clear that nanotechnology is progressing towards the construction of intelligent sensors, actuators, and systems that are smaller than 100 nm. These nanoelectromechanical systems (NEMS) will serve as both the tools to be used for fabricating future nanorobots as well as the components from which these nanorobots may be developed. Shrinking device size to these dimensions presents many fascinating opportunities such as manipulating nano-objects with nanotools, measuring mass in femtogram ranges, sensing forces at piconewton scales, and inducing gigahertz motion, among other new possibilities waiting to be discovered. These capabilities will, of course, drive the tasks that future nanorobots constructed by and with NEMS will perform. NEMS and the components of nanorobots will be the products of nanorobotic manipulation. Large nanorobotic manipulators will be able to shrink in size due to this development, thus enabling nanosized robotic manipulators and other forms of nanorobots. All of these form the scope of the area of nanorobotics.

This chapter focuses on micro- and nanorobotics including actuation, manipulation, and assembly at the micro- and nanoscale. The main goal of these fields of robotics is to provide an effective technology for the experimental exploration of the micro- and nanoworld, and to push the boundaries of this exploration from a robotics research perspective.

18.2 Scaling

18.2.1 The Size of Things

Things we can potentially observable range from 10^{-35} m (the Planck length) to 10^{26} m (the radius of the observable universe). A nanometer, 10^{-9} m, is about ten times the size of the smallest atoms, such as hydrogen and carbon, while a micron is barely larger than the average wavelength of visible light, thus invisible to the human eye. A millimeter, the size of a pinhead, is roughly the smallest part typically fabricated using traditional machining techniques. The range of scales from millimeters to nanometers is one million (Fig. 18.1), which is also about the range of scales in present-day mechanical technology from the largest skyscrapers to the smallest conventional mechanical machine parts. The vast opportunity to make new machines spanning almost six orders of magnitude from 1 mm to 1 nm, is one take on Richard Feynman's famous statement, "there is plenty of room at the bottom" [18.1]. If L is taken as a typical length, 0.1 nm for an atom, perhaps 2 m for a human, this scale range in L would be 2×10^{10}. If the same scale range were to apply to an area, $0.1\,\text{nm}\times0.1\,\text{nm}$ versus $2\,\text{m}\times2\,\text{m}$, the scale range for area L^2 is 4×10^{20}. Since a volume L^3 is enclosed by sides L, we can see that the number of atoms of size 0.1 nm in a $(2\,\text{m})^3$ volume is about 8×10^{30}, recalling that Avogadro's number $N_\text{A}=6.022\times10^{23}$ is the number of atoms in a gram-mole, supposing that the atoms were ^{12}C, molar responding to a density $1.99\times10^4\,\text{kg/m}^3$. A primary working tool of the nanotechnologist is facility in scaling the magnitudes of various properties of interest, as the length scale L shrinks, e.g., from 1 mm to 1 nm.

Clearly, the number of atoms in a device scales as L^3. If a transistor on the micron scale contains 10^{12} atoms, then on the nanometer scale, $L'/L=10^{-3}$ it will contain 1000 atoms, likely too few to preserve its function.

Normally, we will think of scaling as an isotropic scale reduction in three dimensions. However, scaling can be thought of usefully when applied only to one or two dimensions, scaling a cube to a two-dimensional (2-D) sheet of thickness a or to a one-dimensional (1-D) tube or nanowire of cross-sectional area a^2. The term *zero-dimensional* (0-D) is used to describe an object small in all three dimensions, having volume a^3. In electronics, a zero-dimensional object (a nanometer-sized cube a^3 of semiconductor) is called a quantum dot (QD) or *artificial atom* because its electronic states are few and sharply separated in energy, and thus resemble the electronic states of an atom.

18.2.2 Predominate Physics at the Micro- and Nanoscales

The predominate physics at the micro- and nanoscale can be dramatically different from at the macroscale. Surface and intermolecular forces, such as adhesion forces

originating from surface tension forces, van der Waals forces, and electrostatic forces, become more significant than volumetric forces such as gravitational forces for objects with sizes well below 1000 μm [18.22]. Although the laws of classical Newtonian physics may well suffice to describe changes in behavior down to 10 nm (100 Å), the range of scaling is tremendous. Therefore, the changes in magnitudes of many important physical properties, such as resonant frequencies, are so great, that completely different applications may appear.

The more challenging question for the nanotechnologist is to understand and hopefully to exploit those changes in physical behavior that occur at the end of the classical scaling range. The *end of the scaling* is the size scale of atoms and molecules, where nanophysics [18.23] is the proven conceptual replacement of the laws of classical physics. Modern physics, which includes quantum mechanics as a description of matter on a nanometer scale, is a very well-developed and proven subject whose application to real situations is limited only by modeling and computational competence.

In the modern era, simulations and approximate solutions increasingly facilitate the application of nanophysics to almost any problem of interest. Many central problems are already (adequately, or more than adequately) solved in the extensive literatures of theoretical chemistry, biophysics, condensed matter physics, and semiconductor device physics. The practical problem is to find the relevant work, and, frequently, to convert the notation and units systems to apply the results to the problem at hand.

18.3 Actuation at the Micro- and Nanoscales

The positioning of nanorobots and nanorobotic manipulators depends largely on nanoactuators. While nanosized actuators for nanorobots are still under exploration and relatively far from implementation, MEMS-based efforts are focused on shrinking their sizes [18.30]. Nanometer resolution motion has been extensively investigated and can be generated using various actuation principles. Electrostatics, electromagnetics, and piezoelectrics are the most common ways to realize actuation at nanoscales. For nanorobotic manipulation, besides nanoresolution and compact sizes, actuators generating large strokes and high forces are best suited for such applications. The speed criteria are of less importance as long as the actuation speed is in the range of a couple of hertz and above. Table 18.1 provides a small selection of early works on actuators [18.24–29] suitable for micro- and nanorobotic applications (partially adapted from [18.30]).

Several extensive reviews on various actuation principles have been published [18.4, 31–34]. During the design of an actuator, the trade-offs among range of motion, force, speed (actuation frequency), power consumption, control accuracy, system reliability, robustness, load capacity, etc. must be taken into consideration. This section reviews basic actuation technologies and potential applications at nanometer scales.

18.3.1 Electrostatics

Electrostatic charge arises from a build up or deficit of free electrons in a material, which can exert an attractive force on oppositely charged objects, or a repulsive

Table 18.1 Actuation with MEMS

Actuation principle	Type of motion	Volume (mm^3)	Speed (s^{-1})	Force (N)	Stroke (m)	Resolution (m)	Power density (W/m^3)	Ref.
Electrostatic	Linear	400	5000	1×10^{-7}	6×10^{-6}	NA	200	[18.24]
Magnetic	Linear	$0.4\times0.4\times0.5$	1000	2.6×10^{-6}	1×10^{-4}	NA	3000	[18.25]
Piezoelectric	Linear	$25.4\times12.7\times1.6$	4000	350	1×10^{-3}	7×10^{-8}	NA	[18.26]
Actuation principle	**Type of motion**	**Volume (mm^3)**	**Speed (rad/s)**	**Torque (Nm)**	**Stroke (rad)**	**Resolution (rad)**	**Power density (W/m^3)**	**Ref.**
Electrostatic	Rotational	$\pi/4\times0.5^2\times3$	40	2×10^{-7}	2π	NA	900	[18.27]
Magnetic	Rotational	$2\times3.7\times0.5$	150	1×10^{-6}	2π	$5/36\pi$	3000	[18.28]
Piezoelectric	Rotational	$\pi/4\times1.5^2\times0.5$	30	2×10^{-11}	0.7	NA	NA	[18.29]

force on similarly charged objects. Since electrostatic fields arise and disappear rapidly, such devices will likewise demonstrate very fast operation speeds and be little affected by ambient temperatures.

Previous investigations have produced many examples of miniature devices using electrostatic force for actuation including silicon micromotors [18.35,36], microvalves [18.37], and microtweezers [18.38]. This type of actuation is important for achieving nanoscale actuation.

Electrostatic fields can exert great forces, but generally across very short distances. When the electric field must act over larger distances, a higher voltage will be required to maintain a given force. The extremely low current consumption associated with electrostatic devices makes for highly efficient actuation.

18.3.2 Electromagnetics

Electromagnetism arises from electric current moving through a conducting material. Attractive or repulsive forces are generated adjacent to the conductor and proportional to the current flow. Structures can be built which gather and focus electromagnetic forces, and harness these forces to create motion.

Electromagnetic fields arise and disappear rapidly, thus permitting devices with very fast operation speeds. Since electromagnetic fields can exist over a wide range of temperatures, performance is primarily limited by the properties of the materials used in constructing the actuator.

One example of a microfabricated electromagnetic actuator is a microvalve which uses a small electromagnetic coil wrapped around a silicon micromachined valve structure [18.39]. The downward scalability of electromagnetic actuators into the micro- and nanorealm may be limited by the difficulty of fabricating small electromagnetic coils. Furthermore, most electromagnetic devices require perpendicularity between the current conductor and the moving element, presenting a difficulty for planar fabrication techniques commonly used to make silicon devices.

An important advantage of electromagnetic devices is their high efficiency in converting electrical energy into mechanical work. This translates into less current consumption from the power source.

18.3.3 Piezoelectrics

Piezoelectric motion arises from the dimensional changes generated in certain crystalline materials when subjected to an electric field or to an electric charge. Structures can be built which gather and focus the force of the dimensional changes, and harness them to create motion. Typical piezoelectric materials include quartz (SiO_2), lead zirconate titanate (PZT), lithium niobate, and polymers such as polyvinyledene fluoride (PVDF).

Piezoelectric materials respond very quickly to changes in voltages and with great repeatability. They can be used to generate precise motions with repeatable oscillations, as in quartz timing crystals used in many electronic devices. Piezoelectric materials can also act as sensors, converting tension or compression strains to voltages.

On the microscale, piezoelectric materials have been used in linear inchworm drive devices and micropumps [18.40]. STMs and most nanomanipulators use piezoelectric actuators.

Piezoelectric materials operate with high force and speed, and return to a neutral position when unpowered. They exhibit very small strokes (under 1%). Alternating electric currents produce oscillations in the piezoelec-

Table 18.2 Comparison of nanoactuators

Method	Efficiency	Speed	Power density
Electrostatic	Very high	Fast	Low
Electromagnetic	High	Fast	High
Piezoelectric	Very high	Fast	High
Thermomechanical	Very high	Medium	Medium
Phase change	Very high	Medium	High
Shape memory	Low	Medium	Very high
Magnetostrictive	Medium	Fast	Very high
Electrorheological	Medium	Medium	Medium
Electrohydrodynamic	Medium	Medium	Low
Diamagnetism	High	Fast	High

tric material, and operation at the sample's fundamental resonant frequency produces the largest elongation and highest power efficiency [18.41]. Piezoelectric actuators working in the *stick–slip* mode can provide millimeter to centimeter strokes. Most commercially available nanomanipulators adopt this type of actuators, such as Picomotors™ from New Focus and Nanomotors™ from Klock.

18.3.4 Other Techniques

Other techniques include thermomechanical, phase change, shape memory, magnetostrictive, electrorheological, electrohydrodynamic, diamagnetism, magnetohydrodynamic, shape changing, polymers, and biological methods (living tissues, muscle cells, etc.). Table 18.2 compares these techniques.

18.4 Sensing at the Micro- and Nanoscales

A brief overview is given of common imaging tools used in the research area of micro- and nanorobotics including optical, electron, and scanning probe microscopy. The application and integration of these tools for micro- and nanorobotics are discussed in separate sections.

In selecting a proper tool for imaging/sensing at these scales, the following factors should be first considered:

1. Specimen: size, conductivity, and environment compatibility are among the most important aspects to consider. For example, in vivo bioapplications generally require air or liquid, so lower-resolution, light microscopy should be the first choice. If higher resolution is needed, atomic force microscopy or scanning near-field optical microscopy can be used.
2. Resolution: the ability to see fine details of a specimen. Once you can resolve fine details then you can magnify them. Every microscope has a finite resolution; if you magnify objects beyond the resolution the result will be empty magnification. Roughly speaking, a light microscope cannot provide a resolution better than 200 nm. The best commercially available scanning electron microscopes (SEM) have approximately 1 nm resolution, while transmission electron microscopes (TEM) can achieve approximately 0.2 nm, and a scanning tunneling microscope (STM) working in ultrahigh vacuum under very low temperature can resolve atomic-level structures. A comparison of optical microscopy and electron microscopy is given in Table 18.3.
3. Depth of field: the range of depth that a specimen is in acceptable focus. A microscope that has a small depth of field will have to be continuously focused up and down to view a thick specimen.
4. Contrast: the ratio between dark and light. Typically, most microscopes use absorption contrast, i. e., the specimen is subjected to stains in order to be seen. This is called bright-field microscopy. There are other types of microscope that use more exotic means to generate contrast, such as phase contrast, dark field, and differential interference contrast.
5. Brightness: the amount of light. The higher a microscope magnifies the more light will be required. The illumination source should also be at a wavelength (color) that will facilitate interaction with the specimen. All microscopes fall into either of two cat-

Table 18.3 Comparison of optical microscopes and electron microscopes

Feature	OM	TEM	SEM
General use	Surface morphology and sections (1–40 μm)	Section (40–150 nm) or small particles on thin membranes	Surface morphology
Source of illumination	Visible light	High-speed electrons	High-speed electrons
Best resolution	ca. 200 nm	ca. 0.2 nm	ca. 3–6 nm
Magnification range	10–1000 ×	500–500 000 ×	20–150 000 ×
Depth of field	0.002–0.05 nm (N.A. 1.5)	0.004–0.006 mm (N.A. 10^{-3})	0.003–1 mm
Lens type	Glass	Electromagnetic	Electromagnetic
Image ray-formation spot	On eye by lenses	On phosphorescent plate by lenses	On cathode tube by scanning device

egories based on how the specimen is illuminated. In the typical compound microscope the light passes through the specimen and is collected by the image forming optics. This is called diascopic illumination. Dissecting (stereo) microscopes generally use episcopic illumination for use with opaque specimen. The light is reflected onto the specimen and then into the objective lens.

18.4.1 Optical Microscopy

Since their invention in the late 1500s, light microscopes have enhanced our knowledge in basic biology, biomedical research, medical diagnostics, and materials science. Light microscopes can magnify objects up to 1000 times, revealing microscopic details. Light-microscopy technology has evolved far beyond the first microscopes of Robert Hooke and Antoni van Leeuwenhoek. Special techniques and optics have been developed to reveal the structures and biochemistry of living cells. Most optical microscopes in current use are known as compound microscopes, where a magnified image of an object is produced by the objective lens, and this image is magnified by a second lens system (the ocular or eyepiece) for viewing. Microscopes have even entered the digital age, using charge-coupled devices (CCDs) and digital cameras to capture images.

The development of modern microscopy has enabled a large family of optical microscopes. For special purposes, other types of optical microscopes can be selected. These include phase-contrast microscopy, fluorescence microscopy, confocal scanning optical microscopy, and deconvolution microscopy image reconstruction.

18.4.2 Electron Microscopy

Scanning Electron Microscope (SEM)

Since the commercial availability of the SEM in 1966, it has been a valuable resource for viewing samples at a much higher resolution and depth of field than the typical optical microscope. Conventional SEMs can resolve down to the nanometer scale (≈ 1 nm) whereas an optical microscope can only resolve down to approximately 200 nm [18.42]. Unlike conventional optical microscopes, SEMs have a high depth of field which gives imaged samples a three-dimensional appearance. Early SEMs were limited to viewing conductive samples. However, many of today's SEMs can image nonconductive samples in addition to conductive samples using variable-pressure chambers.

Transmission Electron Microscope (TEM)

The TEM can resolve to an atomic scale down to about 1 Å (i. e., 0.1 nm). The TEM mode of operation is similar to that of the SEM in that both microscopes contain an electron gun source of illumination. However, the TEM detects the electrons that pass through a given sample. As a result, the electron gun of the TEM operates at higher energy levels between 50–1000 kV, while the SEM's electron gun operates at around 1–30 kV. In order for proper imaging to take place, the sample must be very thin so that electrons from the beam can pass through the specimen. Electrons that do not pass through the sample cannot be detected. Unlike the SEM, the TEM produces images that are two dimensional in appearance.

18.4.3 Scanning Probe Microscopy

Scanning Tunneling Microscope (STM)

Similar to the TEM, the STM [18.19] can also resolve specimens down to the atomic scale. The scanning probe of the STM is comprised of a noble metal sharpened to an atomic-sized tip, which is mounted on a piezoelectrically driven (x, y, z) linear stage. The STM makes use of the quantum-mechanical effect known as tunneling. Electron tunneling occurs when electrons, driven by a small potential difference, flow across the gap between the probe tip and sample. This event takes place at Ångström-scale distances between the probe tip and the sample [18.43]. The tunneling current, which is typically on the order of a few nanoamperes, is directly related to the tip–sample separation distance. Thus, the tunneling current can be measured and is kept at a constant value by controlling the tip–sample gap distance (z) with a feedback control system. The probe tip is then scanned (x, y) along the entire surface of the sample. Since the control system maintains a constant tunneling current, and thus maintains a constant tip–sample distance (z), the result of a scan yields a $z(x, y)$ terrain map of the sample with enough resolution to detect atomic-scale features. The STM can achieve faster imaging by operating in so-called constant-height mode in which the probe tip is scanned in a plane parallel to the average surface portion. The tip–sample distance (z) can then be inferred directly from the measured tunneling current [18.43].

Atomic Force Microscope (AFM)

The AFM [18.44] is considered to be a spin-off of the STM. One shortcoming of the STM is that it requires conductive probe tips and samples to work properly. The AFM was developed in order to view nonconduc-

tive samples, giving it a wider applicability than the STM. In addition to imaging nonconductive samples, the AFM can also image samples immersed in liquid, which is useful for biological applications [18.45]. Although the STM and AFM are similar in that they both scan the surface of a sample with an atomically sharp probe, they operate under slightly different principles. The AFM is based on interatomic forces as opposed to the electron tunneling used in the STM. The AFM probe tip is mounted on the end of a microscale cantilever beam. At very short separations, the forces between atoms in the probe tip and atoms in the sample cause the cantilever to deflect. This deflection is usually measured by striking the back of the cantilever with a laser. The reflection of the laser beam hits a photodetector, which can be used to recover the deflection of the cantilever. The force can then be calculated by using Hooke's law, which simply relates the applied force to the stiffness and deflection of a material. The forces that are measured can be on the scale of piconewtons [18.43]. The AFM has three main modes of operation known as contact mode, noncontact mode, and tapping mode.

Unlike the SEM and TEM, both the STM and AFM do not require a vacuum environment in order to function. However, a high vacuum is advantageous in order to keep the samples from becoming contaminated from the surrounding environment as well as controlling humidity. In addition, atomic resolution in air is hardly possible with an AFM due to humidity. As a result of humidity, a water film is formed and creates problems because of capillary forces. This can be resolved by operating in vacuum environment or completely in a liquid solution [18.43].

18.5 Fabrication

The design of micro- and nanorobotic devices is inextricably linked to available fabrication techniques. However, though the development of microfabrication processes has become somewhat stable over the past decade, nanofabrication processes are still being actively pursued, and the design constraints generated by these processes are relatively unexplored. This section will briefly highlight the processes used in conventional microfabrication including lithography, thin-film deposition, chemical etching, and electrodeposition, and describe some emerging techniques for nanofabrication.

Most micro- and nanofabrication techniques have their roots in the standard fabrication methods developed for the semiconductor industry [18.46–48]. Therefore, a clear understanding of these techniques is necessary for anyone embarking on a research and development path in the micro/nano area.

18.5.1 Microfabrication

In this section, we will discuss the major microfabrication techniques used most frequently in the manufacturing of microstructures.

Photolithography

Lithography is the technique used to transfer a computer-generated pattern onto a substrate (silicon, glass, GaAs, etc.). This pattern is subsequently used to etch an underlying thin film (oxide, nitride, etc.) for various purposes (doping, etching, etc.). Although photolithography, i. e., lithography using an ultraviolet (UV) light source, is by far the most widely used lithography technique in microelectronic fabrication, electron-beam (e-beam) and X-ray lithography are two alternatives that have attracted considerable attention in the MEMS and nanofabrication areas. We will discuss photolithography in this section and postpone the discussion of e-beam and X-ray techniques to the subsequent sections dealing with nanofabrication.

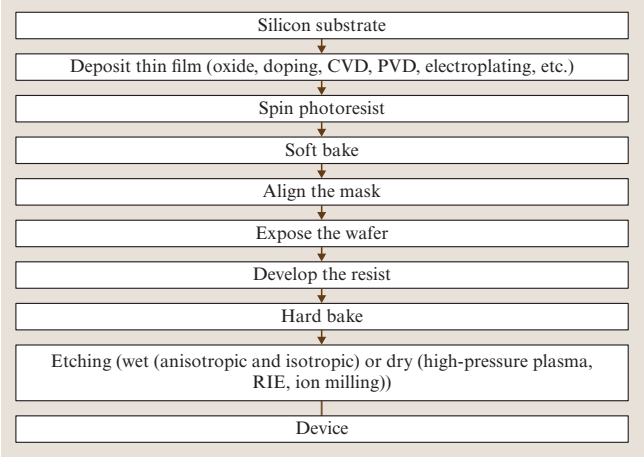

Fig. 18.2 Typical microfabrication process flow

The starting point following the creation of the computer layout for a specific fabrication sequence is the generation of a photomask. This involves a sequence of photographic processes (using optical or e-beam pattern generators) that results in a glass plate having the desired pattern in the form of a thin (≈ 100 nm) chromium layer. Following the generation of photomask, the lithography and etching process can proceed as shown in Fig. 18.2. After depositing the desired material on the substrate, the photolithography process starts with spin-coating the substrate with a photoresist. This is a polymeric photosensitive material that can be spun onto the wafer in liquid form; usually an adhesion promoter such as hexamethyldisilazane (HMDS) is used prior to the application of the resist. The spinning speed and photoresist viscosity will determine the final resist thickness, which is typically 0.5–2.5 μm. Two different kinds of photoresist are available: positive and negative. With a positive resist, the UV-exposed areas will be dissolved in the subsequent development stage, whereas with a negative photoresist, the exposed areas will remain intact after the development. After spinning the photoresist on the wafer, the substrate is soft-baked (5–30 min at 60°–100 °C) in order to remove the solvents from the resist and improve the adhesion. Subsequently, the mask is aligned to the wafer and the photoresist is exposed to a UV source.

After exposure, the photoresist is developed in a process similar to the development of photographic film. The resist is subsequently hard-baked (20–30 min at 120°–180 °C) in order to further improve the adhesion. The hard-bake step concludes the photolithography sequence by creating the desired pattern on the wafer. Next, the underlying thin film is etched, and the photoresist is stripped in acetone or other organic solvent. Figure 18.3 shows a schematic of the photolithography steps with a positive photoresist.

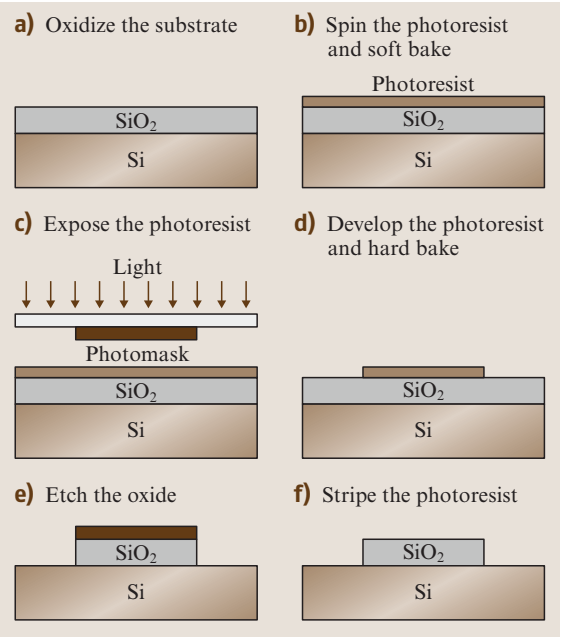

Fig. 18.3a–f Schematic drawing of the photolithographic steps with a positive photoresist (PR)

Thin-Film Deposition and Doping

Thin-film deposition and doping are used extensively in micro- and nanofabrication technologies. Most of the fabricated structures contain materials other than that of the substrate, which are obtained by various deposition techniques, or by modification of the substrate. These techniques include oxidation, doping, chemical vapor deposition (CVD), physical vapor deposition (PVD), and electroplating.

Etching and Substrate Removal

For micro- and nanofabrication, in addition to thin film etching, often the substrate (silicon, glass, GaAs, etc.) needs to be removed in order to create various mechanical structures (beams, plates, etc.). Two important figures of merit for any etching process are selectivity and directionality.

Selectivity is the degree to which the etchant can differentiate between the masking layer and the layer to be etched. Directionality has to do with the etch profile under the mask. In an isotropic etch, the etchant attacks the material in all directions at the same rate, creating a semicircular profile under the mask (Fig. 18.4a). In an anisotropic etch, the dissolution rate depends on specific directions, and one can obtain straight sidewalls or other noncircular profiles (Fig. 18.4b). One can also divide the various etching techniques into wet and dry categories. Due to the lateral undercut, the minimum feature size achievable with wet etchants is limited to > 3 μm. Photoresist and silicon nitride are the two most common masking materials for the wet oxide etch. Anisotropic and isotropic wet etching of crystalline (silicon and gallium arsenide) and noncrystalline (glass) substrates are important topics in micro- and nanofabrication [18.49–53].

The anisotropic behavior of these etchants with respect to the (111) planes have been used extensively to create beams, membranes, and other mechanical and structural components. Figure 18.5 shows the typical

cross sections of (100) silicon wafers etched with an anisotropic wet etchant. As can be seen, the (111) slow planes are exposed and creating 54.7° sloped sidewalls. Depending on the dimensions of the mask opening, a V-groove or a trapezoidal trench is formed in the (100) wafer. A large enough opening will allow the silicon to be etched all the way through the wafer, thus creating a thin dielectric membrane of the other side. It should be mentioned that exposed convex corners have a higher etch rate than the concave ones, resulting in an undercut that can be used to create dielectric (e.g., nitride) cantilever beams.

Dry etching techniques are largely plasma based. They have several advantages compared with wet etching. These include smaller undercut (allowing smaller lines to be patterned) and higher anisotropy (allowing high-aspect-ratio vertical structures). However, the selectivity of dry etching techniques is lower than the wet etchants, and one must take into account the finite etch rate of the masking materials. The three basic dry etching techniques, namely high-pressure plasma etching, reactive-ion etching (RIE), and ion milling, utilize different mechanisms to obtain directionality.

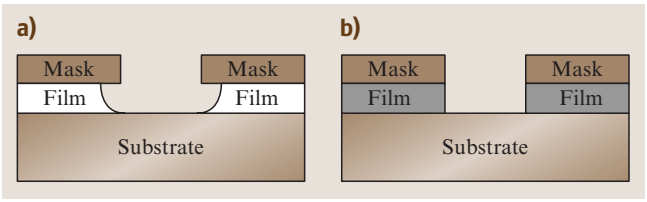

Fig. 18.4a,b Profile for isotropic **(a)** and anisotropic **(b)** etch through a photoresist mask

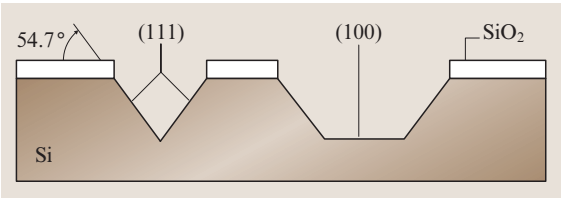

Fig. 18.5 Anisotropic etch profiles for (100) silicon wafers

18.5.2 Nanofabrication

The design and fabrication of NEMS is an emerging area being pursued by an increasing number of researchers. Two approaches to nanofabrication, top-down and bottom-up, have been identified by the nanotechnology research community and are being independently investigated by various researchers. Top-down approaches are based on microfabrication and include technologies such as nanolithography, nanoimprinting, and chemical etching. Presently, these are 2-D fabrication processes with relatively low resolution. Bottom-up strategies are assembly-based techniques. Currently these strategies include techniques such as self-assembly, dip-pen lithography, and directed self-assembly. These techniques can generate regular nanopatterns at large scales.

In this section, we will discuss three major nanofabrication techniques. These include:

1. e-beam and *nanoimprint* fabrication,
2. *epitaxy* and *strain engineering*, and
3. dip-pen nanolithography.

E-beam Lithography and Nanoimprint Fabrication

In previous sections, we discussed several important lithography techniques commonly used in MEMS and microfabrication. These include various forms of UV (regular, deep, and extreme) and X-ray lithography. However, due to the lack of resolution (in the case of the UV), or the difficulty in manufacturing mask and radiation sources (X-ray), these techniques are not suitable for nanometer-scale fabrication. E-beam lithography is an attractive alternative technique for fabricating nanostructures [18.53]. It uses an electron beam to expose an electron-sensitive resist such as polymethyl methacrylate (PMMA) dissolved in trichlorobenzene (positive) or polychloromethylstyrene (negative).

The e-beam gun is usually part of an SEM, although a TEM can also be used. Although electron wavelengths on the order of 1 Å can easily be achieved, electron scattering in the resist limits the attainable resolutions to > 10 nm. The beam control and pattern generation are achieved through a computer interface.

E-beam lithography is serial and hence has a low throughput. Although this is not a major concern in fabricating devices used in studying fundamental microphysics, it severely limits large-scale nanofabrication. E-beam lithography, in conjunction with such processes as lift-off, etching, and electrodeposition, can be used to fabricate various nanostructures.

An interesting new technique that circumvents the serial and low-throughput limitations of the e-beam lithography for fabricating nanostructures is nanoimprint technology [18.54]. This technique uses an e-beam-fabricated hard material master (or mold) to stamp and deform a polymeric resist. This is usually followed by a reactive-ion etching step to transfer the stamped pattern to the substrate. This technique is eco-

nomically superior, since a single stamp can be used repeatedly to fabricate a large number of nanostructures.

Epitaxy and Strain Engineering

Atomic-precision deposition techniques such as molecular-beam epitaxy (MBE) and metallo-organic chemical vapor deposition (MOCVD) have proven to be effective tools in fabricating a variety of quantum confinement structures and devices (quantum well lasers, photodetectors, resonant tunneling diodes, etc.) [18.55–57].

Dip-Pen Nanolithography

In dip-pen nanolithography (DPN), the tip of an AFM operated in air is *inked* with a chemical of interest and brought into contact with a surface. The ink molecules flow from the tip onto the surface as with a fountain pen. Line widths down to 12 nm with spatial resolution of 5 nm have been demonstrated with this technique [18.58]. Species patterned with DPN include conducting polymers, gold, dendrimers, deoxyribonucleic acid (DNA), organic dyes, antibodies, and alkanethiols.

18.6 Microassembly

Assembly is often required in macroscale product manufacturing in order to reduce the complexity and cost of the manufacturing process. Assembly makes it possible to build complex products from relatively simple parts and to integrate incompatible manufacturing processes. It also makes maintenance and replacement possible. The extension of assembly techniques into the microscale is driven by the development of modern design and manufacturing technologies in the pursuit of miniaturization and function integration, especially by the development of integrated circuit (IC) [18.59] and MEMS fabrication techniques. With the extension of manufacturing technology into the microscale and even nanoscale domain, the term microassembly has been created to refer specifically to assembly operations performed at the micro/mesoscale [18.60]. To give a formal definition, microassembly is the assembly of objects with microscale and/or mesoscale features under microscale tolerances [18.61].

18.6.1 Automated Microassembly Systems

Microassembly plays the role of an enabling technology in various processes of MEMS fabrication, including device fabrication, packaging, and interconnection. MEMS device fabrication is fundamentally different from the highly modular IC fabrication in that it often requires the machining of complex-shaped 3-D mechanical structures [18.51]. However, almost all current MEMS fabrication techniques are subject to constraints in limited allowable materials, limited capabilities in true 3-D fabrication, and the requirement of fabrication process compatibility. Microassembly provides a possible solution to these constraints. For example, incompatible fabrication processes can be integrated through assembly. This makes it possible to use *nontraditional* fabrication techniques that are not necessarily based on semiconductor materials, such as laser cutting, microwire electrical discharge machining (EDM), and micromilling [18.62]. Complex 3-D structures can also be developed using parts with relatively simple geometry [18.63, 64]. Microassembly is also crucial to MEMS packaging and interconnection [18.65, 66].

From the perspective of robotic systems and automation, MEMS device fabrication and packaging share many common assembly requirements. A fundamental commonality of both processes is the requirement of the ability to manipulate micro/mesoscale objects so that precise (i. e., microscale tolerance) spatial relations can be established (e.g., die alignment, part insertion) and certain physical/chemical processes (e.g., die bonding, surface coating) can be performed. Another common requirement is to control the interaction force involved. MEMS devices often have fragile structures such as thin beams or membranes. This requires controlling the interactive force in manipulation operations. Typically, the force magnitude resides in the range from millinewtons to micronewtons.

MEMS devices are often three-dimensional. MEMS packaging requires both electrical interconnection for signal transmission and mechanical interconnection for the interaction of the packaged device with its external environment [18.51, 67]. Many such mechanical interconnections require three-dimensional manipulation and three-dimensional force control. The actual operations are highly application specific, which pose great challenges to the development of automated microassembly systems. Automated IC packaging systems can be used for the packaging of certain MEMS devices such as accelerometers and gyros. However, packaging of mi-

crofluidic devices, optical MEMS devices, and hybrid microsystems often require the development of new automated microassembly techniques and systems.

The selection of assembly mode is among the first decisions to be made in developing automated microassembly systems. Sequential microassembly requires the use of micromanipulators and sensory feedback. At each moment, only one or a few parts are being assembled. Depending on the physical effects used, parallel microassembly can be either deterministic or stochastic [18.68]. Die bonding is an example of deterministic parallel microassembly. In stochastic parallel microassembly, large numbers of parts are assembled simultaneously using distributed physical effects such as electrostatic force, capillary force, centrifugal force, or vibration [18.60, 69–71]. In fact, the basic philosophy of stochastic parallel microassembly is to minimize the use of sensory feedback.

Each of these assembly modes has both advantages and disadvantages. Each has its own suitable applications. Deterministic parallel assembly shares several commonalities with sequential microassembly. For example, sensory feedback is often used in deterministic parallel microassembly. However, deterministic parallel microassembly requires high relative positioning accuracy between parts. In addition, only simple planar structure features can be assembled in order to make parallel operation possible.

Due to the requirement of MEMS packaging for three-dimensional manipulation and microassembly, it can be expected that automated sequential microassembly will be the most widely adopted solution. In particular, those MEMS packaging applications that require the control of multiple-degree-of-freedom (DOF) interaction force should use sequential microassembly. The major possible disadvantage of sequential microassembly is its low throughput. This constraint can often be overcome by appropriate system design.

Here we introduce a three-dimensional microassembly example that originates from an industrial application [18.61]. It is significantly different from wire bonding and die bonding applications in that high-precision 3-D part insertion is required. Together with other examples, it will be used throughout this section to illustrate the major concepts and techniques and the logic connections between each functional unit of an automated microassembly system.

The assembly task is to pick up micromachined thin metal parts that are transferred to the assembly workcell on a vacuum-release tray (Fig. 18.6a, b and c), and insert them into vertically deep reactive ion etching (DRIE) etched holes in a silicon wafer (Fig. 18.6d). The wafers can have diameters up to 8 inches. The holes on each wafer form regular arrays consisting of approximately 50 holes each. However, these arrays may not be regularly distributed on the wafer. Typically, hundreds of parts are to be assembled on each wafer. In general, each assembly operation is a typical rectangular-peg-into-a-rectangular-hole problem. Each metal part is approximately half a millimeter in width and less than 100 μm in thickness at its rectangular tip. The total assembly tolerance is typically smaller than 10 μm in the vertical direction, and smaller than 20 μm in the horizontal direction. This task is a typical application of 3-D microassembly techniques.

18.6.2 Microassembly System Design

This section discusses the design of automated microassembly systems from the perspective of robotic systems and automation. Performance objects to be achieved include high reliability, high throughput, high flexibility, and low cost.

General Guidelines

Taking a system perspective. An automated microassembly system consists of many functional units and must integrate techniques from a diverse range of areas such as robotics, computer vision, microscope op-

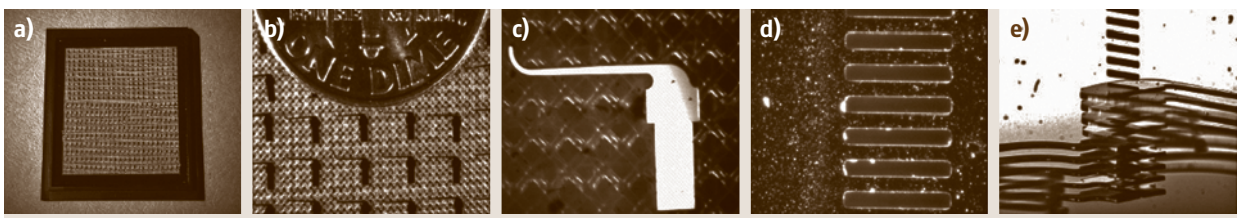

Fig. 18.6a–e A 3-D microassembly example

tics, physics, and chemistry. It is therefore important to consider the interaction between these units.

Emphasizing the coupling with packaging processes. Although in this section microassembly techniques are addressed primarily from the perspective of robotics for the clarity of presentation, robotic system designers must recognize the strong dependence of architecture design of the robotic systems on the packaging process being implemented. This connection should be emphasized from the beginning of system development.

Design for reconfigurability. Automated packaging machines must be designed so that they can be customized for a wide variety of applications. Reconfigurability is therefore a basic design requirement. Typically, modular design based on function decomposition is desirable. Support for tool replacement is essential.

The design of automated microassembly systems is strongly dependent on the assembly tolerance required. First of all, the repeatability of the motion control system and the micromanipulator used is determined by the required assembly tolerance. In addition, assembly tolerance often determines the minimum resolution of the microscope optics. General microassembly tasks may only require microscopic vision feedback and manipulators with microscale repeatability, while complex microassembly tasks may also require the integration of microforce and vision feedback [18.72, 73].

Automated microassembly systems must be able to support a wide variety of material-handling tools, which include part transfer tools, bulk feeders, wafer-handling tools, magazine loaders and unloaders, etc.

The role of the micromanipulator is to provide multiple-DOF fine motion control. The role of the microgripper is to grasp objects in pick-and-place and other assembly operations. Their efficiency and robustness will to a great extent decide the performance of the entire system. Microgripper design is also closely related to the design of fixtures for microassembly operations.

Major environment factors include clean-room requirements, temperature, humidity, airflow, etc. Certain assembly operations must be performed in a clean room. This requires that the design of automated microassembly systems comply with relevant standards. Some packaging processes such as eutectic bonding must be performed under high temperature. Consequently, the potential influence of high temperature on motion control system and microscope optics must be considered. For the manipulation of microscale objects, environment conditions such as temperature and humidity can have a major influence on adhesion forces [18.74, 75]. Therefore, it is often important to consider environment control in system design.

Assembly Process Flow: An Example

The micromachined metal parts (Fig. 18.6c) are horizontally transferred to the workcell on the vacuum-release tray (Fig. 18.6b). The wafer is placed on a wafer mount perpendicular to the horizontal plane (Fig. 18.6b). This configuration does not require the flipping of the thin metal parts and is advantageous in terms of reliability and efficiency. There are two major operations in each assembly cycle: pickup and insertion. Under the configuration shown in Fig. 18.7a, all the operations are performed by the same workcell. Complex packaging operations must often be decomposed and performed by multiple workcells [18.76].

General System Architecture

An automated microassembly system typically consists of the following functional units.

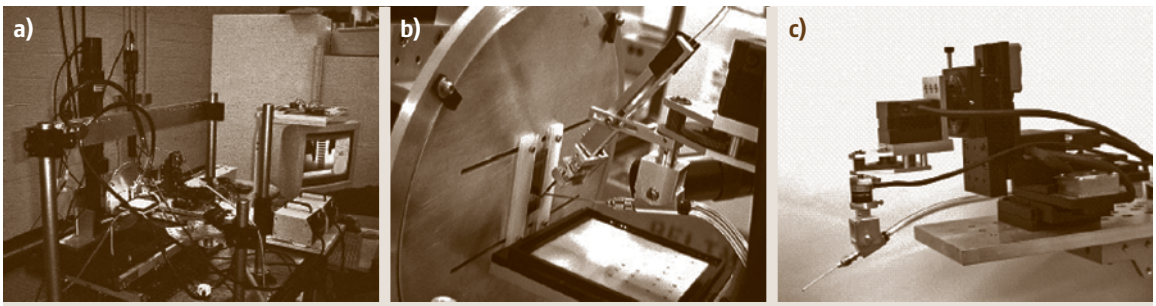

Fig. 18.7a–c An experimental microassembly workcell

Large workspace positioning unit. A large workspace and long-range positioning motion are required in most microassembly operations. The large workspace is necessary to accommodate different functional units, part feeders, and various tools.

In general, off-the-shelf motion control systems developed for automated IC packaging equipment can be adopted directly. For the task described in Sect. 18.6.1, the DRIE-etched holes are distributed on wafers up to 8 inches in diameter. This requires the assembly system to have a commensurate working space and high positioning speed. The coarse positioning unit has four DOFs (Fig. 18.7a). Planar motion in the horizontal direction is provided by an open-frame high-precision XY table with a travel of 32 cm (12 inch) and a repeatability of 1 μm in both directions. Position feedback with a resolution of 0.1 μm is provided by two linear encoders. A dual-loop PID plus feedforward control scheme is used for each axis. The internal speed loop is closed on the rotary encoder on the motor. The external position loop is closed on the linear encoder. Each wafer is placed on the vertical wafer mount that provides both linear and rotational control (Fig. 18.7b). Vertical motions of the wafer mount are provided by a linear slide with a travel of 20 cm (8 inch) and a repeatability of 5 μm. It is also controlled using a PID plus feedforward algorithm. Both the XY table and the vertical linear slides are actuated using alternating-current (AC) servo motors. The rotation of the wafer mount is actuated by an Oriental PK545AUA microstep motor with a maximum resolution of 0.0028°/step. All low-level controllers are commanded and coordinated by a host computer [18.61].

For applications requiring repeatability of one micron or greater, it is convenient to use conventional positioning tables to implement coarse range motions. These tables typically use leadscrew or ballscrew drives and ball or roller bearings. For applications requiring submicron or nanometer repeatability, a few solutions are also commercially available. For example, piezoactuators are often used for nanometer repeatability motion. The disadvantage of piezoactuators is that their travel range is small, typically on the order of 100 microns. As another example, a series of positioning stages with submicron repeatability based on direct-drive linear actuators and air bearings is available from Aerotech. It is also possible to use parallel structure mechanisms such as a Stewart platform [18.77]. In general, the development of IC manufacturing towards the deep submicron level provides a major driving force behind the development of these motion control techniques.

Micromanipulator unit. Fine pose (position and orientation) control is required in operations such as 3-D precision alignment and assembly. For example, the six DOFs required by the task introduced in Sect. 18.6.1 are implemented on separate structures. The three Cartesian DOF are provided by an adapted Sutter MP285 micromanipulator, which also provides yaw motions with its rotational DOF (Fig. 18.7c). Roll motions are implemented on the wafer mount (Fig. 18.7b). The pitch movement of the metal part after pickup is not motorized and is implemented through manual adjustment and calibration before assembly. More discussion of micromanipulator configuration can be found in [18.61].

Two principles need to be considered in implementing motion control for automated 3-D microassembly. The first is the partition of large-workspace coarse positioning unit and the fine positioning micromanipulator unit. The second is the decomposition and distributed implementation of multiple DOFs. In practice, the actual implementations of these principles are highly application specific. For certain applications, if a large-range positioning unit is sufficient to satisfy assembly tolerance requirements, the separate implementation of a micromanipulator may even be unnecessary.

In general, the separation of a micromanipulator unit will facilitate the implementation of high-bandwidth motion control. However, this separation normally brings redundancy to the entire motion control system. The functioning of the high-precision micromanipulator must also rely on closed-loop feedback control, especially microscopic vision feedback.

Automated microgripper unit. The function of a microgripper is to provide geometrical and physical constraints (grasping) in pick-and-place and assembly operations. The reliability and efficiency of the microgripper is critical to the performance of the entire automated microassembly system. Several factors must be considered in micromanipulator design. First of all, as the micromanipulator end-effector, the microgripper must be constantly monitored under a microscope. Therefore, it must be small in size and suitable in shape to remain in the microscope's field of view and to minimize occlusion. Secondly, it is important to consider the different governing physics and to explore the use of various gripping forces [18.77]. Thirdly, microgrippers are used in both part pick-and-place and assembly. Since assembly operations typically require more constraints, microgrippers designed for pick-and-place operations may not necessarily be suitable for assembly operations. In fact, the microassembly task described in Sect. 18.6.2

is performed using a combined microgripper [18.61]. Microgripper development is often closely related to the development of fixtures that can also have microscale sizes.

Microscope optics and imaging unit. The function of the microscope optics and imaging unit is to provide noncontact measurement of the geometry, motion, and spatial relations of assembly objects. Typical configurations of commercial device bonding systems use one or two vertical microscopes. An inverted microscope configuration is commonly used for backside alignment. On the other hand, 3-D microassembly may require two camera views in a stereo configuration. In the system shown in Fig. 18.7a, a total of four different views can be provided to its human operator: a global view of the entire assembly scene, a vertical microscopic view for part pickup, and two lateral microscopic views for the fine position and orientation adjustments during the final microassembly operations. Each view uses a CCD camera with a matching optical system. All images are captured using a Matrox Corona PCI frame grabber.

Microscopic visual feedback is crucial for precise 3-D alignment. Provided that resolution requirements of the assembly task can be satisfied, microscope optics with larger working distances is desirable. For the assembly task addressed in Sect. 18.6.1, an Edmund Scientific VZM 450i zoom microscope with a 1× objective is used to provide the right view. Its working distance is approximately 90 mm, with a resolution of 7.5 μm. The vertical view is also provided by a VZM 450i microscope with a 0.5× objective to guide pickup operations. Its field of view can range from 2.8 × 2.8 mm to 17.6 × 17.6 mm. Its working distance is approximately 147 mm.

If visual servoing is required in automate assembly operations, a stereo configuration formed by adding another lateral view may be necessary. Higher resolution may be necessary in some microassembly tasks. In such cases, the same configuration can be used with higher-resolution microscope optics, for example, two Navitar TenX zoom microscopes with Mitutoyo ultralong-working-distance M Plan Apo 10× objectives have been used in this configuration by the authors. The resolution of each microscope is 1 μm, with a working distance of 33.5 mm. Consequently, the usable workspace of the micromanipulator is reduced [18.61].

The global view is implemented using a miniature Marshall V-1260 board camera to monitor the status of the entire assembly scene. It plays an important role in helping the operator to understand gross spatial relations and preventing operation errors.

From the perspective of robotic systems, the development of automation microassembly systems for complex 3-D microassembly operation will rely on the development of:

1. Compact, robust and high-speed micromanipulators with 5–6 DOFs.
2. Highly reliable and efficient microgrippers that are suitable for working under microscopes. Such grippers should have active force control or passive compliance to avoid damage to MEMS devices.
3. Three-dimensional microscopic computer vision techniques, three-dimensional microforce measurement and control techniques, and their integration.

18.6.3 Basic Microassembly Techniques

This section introduces a few supporting techniques important to automated microassembly systems, including machine vision techniques, microforce control techniques, and simulation verification of assembly strategy.

Machine Vision Techniques

Machine vision techniques are widely used in the semiconductor industry. The major difference between machine vision and general computer vision [18.78] is that, unlike natural objects and scenes, industrial objects and scenes can often be artificially designed and configured. This advantage often makes it possible to significantly reduce the complexity and enhance the robustness of vision techniques. The applications of machine vision techniques can generally be categorized into the following two classes based on the requirement of real-time processing.

Non-time-critical vision applications. These applications do not require visual feedback for high-bandwidth real-time control. Examples include object recognition and packaging quality inspection [18.79].

Time-critical vision applications. These applications require real-time visual feedback. Examples include vision-guided pick-and-place, alignment, insertion, etc. [18.80]. An introduction to 3-D computer vision techniques can be found in [18.81]. A standard introduction to visual servoing techniques can be found in [18.82].

Several commercial software packages are available from suppliers such as Cognex, Coreco Imaging, and National Instruments.

Microforce Control Techniques

The theory of force control has been studied by the robotics community for more than 50 years [18.83, 84]. Several theoretical frameworks and many control algorithms have been proposed and experimentally verified. A variety of macroscale multiple-DOF force sensors have been developed.

Force control is also crucial to microassembly. For example, contact forces in device bonding must often be programmed and precisely controlled. In general, many of the macroscale force control techniques can be applied at micro/mesoscales. Force control for device bonding is essentially 1-D and involves force on the order of several newtons. On the other hand, in the manipulation of micro/mesoscale parts, the magnitude of interactive force typically ranges from millinewtons (10^{-3} N) to micronewtons (10^{-6} N). Forces of this magnitude are often referred to as *microforces*. A major technical challenge in implementing microforce control is the lack of multiple-DOF microforce sensors. A basic requirement for multiple-DOF microforce sensors is that they must be miniature in size. The manufacturing of these sensors normally requires the use of micromachining, including MEMS techniques. There are two major microforce sensing configurations.

Stand-alone force sensor. The advantage of this configuration is that the sensor is general purpose and can be used with different microgrippers. Most macroscale multiple-DOF force sensors are of this type. However, this also requires the sensor to have sufficient structural stiffness to support the static load of microgripper, which is often significantly larger than the force resolution to be reached.

Embedded force sensor. Micro strain gages can be attached to microgrippers [18.85]. Force-sensitive materials can also be deposited on microgrippers. This configuration avoids the issue of static load. However, such force sensing capabilities are dependent on the microgripper design, which often is not necessarily optimal for the measurement of multiple-DOF microforce/torque.

Complex and high-precision microassembly tasks also require the integration of microscopic machine vision with microforce control. Simple integration techniques use a gating/switching scheme [18.72, 86]. For more integrated approaches, visual impedance can be used [18.73].

Simulation Verification of Assembly Strategies

In many microassembly tasks, the distances between adjacent features are often on the meso/microscale. Therefore, selecting the correct assembly sequence is important for collision avoidance. In addition, due to the limited working distance of microscopes, microassembly operations must often be performed in a limited space using micromanipulators. Collision avoidance is critical to avoiding equipment or device damage. Potential collisions can be found and avoided by using offline simulation software. Many commercially available offline robot programming tools can provide this function.

Microassembly Tool

The end-effector of a micromanipulator in an automated microassembly system is often in the form of a microgripper, whose reliability and efficiency greatly influence the reliability and efficiency of the entire system. The microgripper must often be as small as possible. Its design must also minimize potential damage to fragile MEMS parts. This often requires passive compliance in structural design.

Microgrippers with integrated MEMS actuators can be fabricated monolithically and thus can be more compact in size. Several physical effects are commonly used in MEMS actuators, including electrostatic force and piezoelectric force [18.87], SMA (shape memory alloy) [18.88, 89], and thermal deformation [18.63, 90]. Currently, the major limitation is that it is difficult for MEMS actuators to generate sufficient travel, force, and power output. Alternatively, another solution is to provide actuation externally [18.61, 91] The advantage is that sufficient travel and force and power output can be more easily obtained. The major disadvantage is that the microgripper is less compact in size. This could become a major obstacle to its applications.

18.7 Microrobotics

Today, more and more microrobotic devices are enabling new applications in various fields. Besides microassembly, microrobotics can play important roles in other industry fields for manipulation, characterization, in-

spection, and maintenance, and in biotechnology for, e.g., manipulating cells, a field referred to as biomicrorobotics.

18.7.1 Microrobots

Microrobotics is a field that combines the established theory and techniques of robotics with the exciting new tools provided by MEMS technology in order to create intelligent machines that operate at micron scales. As stated by authors reviewing the microrobotics field [18.31, 92], many *micro* terms such as *micromechatronics*, *micromechanism*, *micromachines*, and *microrobots* are used synonymously to indicate a wide range of devices whose function is related to a *small* scale; however, *small* scale is a relative term so a clearer definition is needed.

The obvious difference between a macrorobot and a microrobot is the size of the robot. Thus, one definition of a microrobot is *a device having dimensions smaller than classical watch-making parts (i. e.,* μm *to* mm*) and having the ability to move, apply forces and manipulate objects in a workspace with dimensions in the micrometer or submicrometer range* [18.94]. However, in many cases it is important that the robot can move over much larger distances. This task-specific definition is quite wide and includes several types of very small robots as well as stationary micromanipulation systems, which are a few decimeters in size but can carry out very precise manipulation (in the micron or even nanometer range) [18.92].

Besides classification by task or size, microrobots can also be classified by their mobility and functionality [18.31, 93]. Many robots usually consist of sensors and actuators, a control unit, and an energy source.

Depending on the arrangement of these components, one can classify microrobots according to the following criteria: locomotive and positioning possibility (yes or no), manipulation possibility (yes or no), control type (wireless or tethered), and autonomy. Figure 18.8 illustrates 15 different possible microrobot configurations by combining the four criteria [18.31, 93].

As depicted in Fig. 18.8 (taken from [18.30]), the classification is dependent on the following microrobot components: the control unit (CU), the power source (PS), the actuators necessary for moving the robot platform (i. e., the robot drive for locomotion and positioning; AP), and the actuators necessary for operation (i. e., manipulation using robot arms and hands; AM). Besides the different actuation functions, sensory functions are also needed, for example, tactile sensors for microgrippers or charge-coupled device (CCD) cam-

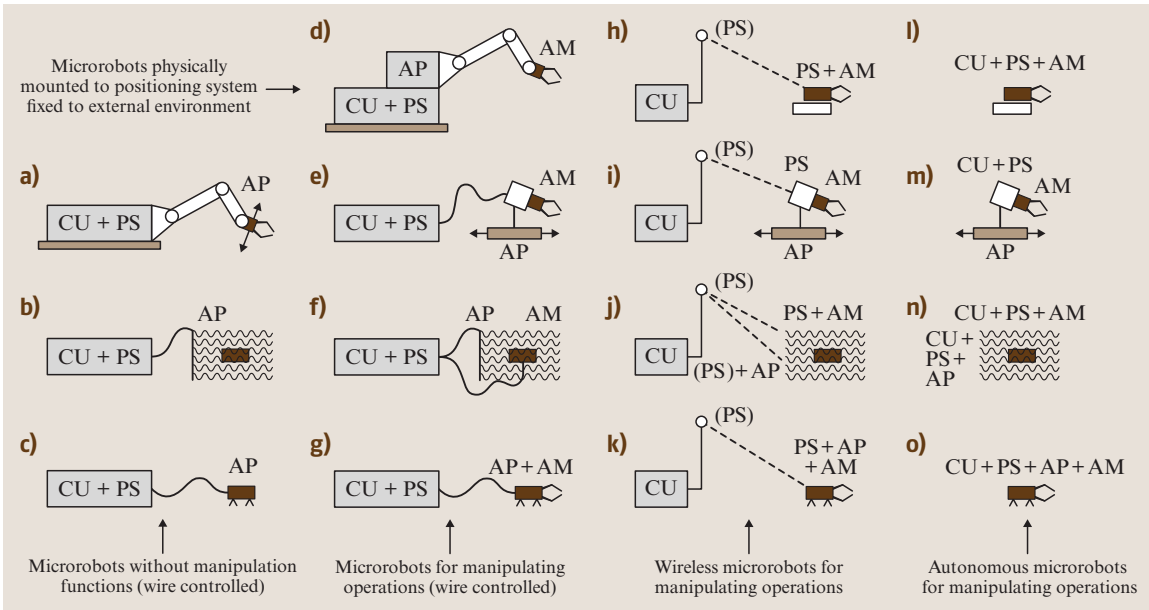

Fig. 18.8a–o Classification of microrobots by functionality (modification of earlier presented classification schemes [18.12, 31, 92, 93]). (CU indicates the control unit; PS, the power source or power supply; AP, the actuators for positioning; AM, the actuators for manipulation)

eras for endoscopic applications (compare Fig. 18.8d and a).

The ultimate goal is to create a fully autonomous, wireless mobile microrobot equipped with suitable microtools according to Fig. 18.8o. Because this is a very difficult task, a good start is to investigate the possibility of making silicon microrobot platforms that are steered and powered through wires, like the one in Fig. 18.8c, and to study their locomotion capability.

The majority of MEMS-based microrobotic devices developed so far could be categorized as moveable links – microcatheters [18.95, 96], according to Fig. 18.8a, or microgrippers [18.24], such as those in Fig. 18.8d, or the microgrippers [18.97, 98] shown in Fig. 18.8e. Among the research publications covering locomotive microrobots, most publications have addressed microconveyance systems (Fig. 18.8b) [18.99–102]. Robots using external sources for locomotion could be used (compare Fig. 18.8b,f,j,n). According to *Fatikow* and *Rembold* [18.92], several researchers are working on methods to navigate micromechanisms through human blood vessels; however, these microrobots are difficult to control. Examples of partially autonomous systems (compare Fig. 18.8j) are the concept for so-called *smart pills*. Centimeter-sized pills for sensing temperature and/or pH inside the body have been presented [18.103, 104] as well as pills equipped with video cameras [18.105]. The pill is swallowed and transported to the part of the body where one wants to measure or record a video sequence. The information of the measured parameter or the signals from the camera is then transmitted (telemetrically) out of the body. More sophisticated approaches involving actuators for drug delivery of various kinds have also been proposed [18.92, 104]. The position of the pill inside the body is located by an X-ray monitor or ultrasound. As soon as the pill reaches an infected area, a drug encapsulated in the pill can be released by the actuators onboard. External communication could be realized through radio signals.

Several important results have been presented regarding walking microrobots (Fig. 18.8c,g,k) fabricated by MEMS technologies and batch manufacturing. Different approaches for surface-micromachined robots [18.106, 107] and for a piezoelectric dry-reactive-ion-etched microrobot should be mentioned. A suitable low-power application-specific integrated circuit (ASIC) for robot control has been successfully tested and is planned to be integrated on a walking microrobot [18.108]. The large European Esprit project *MINIMAN* (1997) has the goal of developing moveable microrobotic platforms with integrated tools with six degrees of freedom for applications such as microassembly within an SEM and involves different MEMS research groups from several universities and companies across Europe. Further, miniature robot systems with MEMS/MST (MicroSystem Technology) components have been developed [18.109].

Several research publications on *gnat* minirobots and actuator technologies for MEMS microrobots [18.3, 110] were reported by US researchers in the early 1990s, and several groups in Japan are also currently developing miniaturized robots based on MEMS devices [18.8]. In Japan, an extensive ten-year program on *micromachine technology,* supported by the Ministry of International Trade and Industry (MITI), started in 1991. One of the goals of this project is to create microsized and miniature robots for microfactory, medical technology, and maintenance applications. Several microrobotic devices, including locomotive robots and microconveyers, have been produced within this program. Miniature robot devices or vehicles [18.111] for locomotive tasks, containing several MEMS components, have been presented. Even though great efforts have been made on robot miniaturization using MEMS technologies, no experimental results on MEMS batch-fabricated microrobots suitable for autonomous walking (i. e., robust enough to be able to carry its own power source or to be powered by telemetric means) have been presented yet. The first batch-fabricated MEMS-based microrobot platform able to walk was presented in 1999 [18.112]. However, this robot was powered through wires and was not equipped with manipulation actuators. Besides walking microrobotic devices, several reports on flying [18.113–115] and swimming [18.116] robots have been published. Micromotors and gear boxes made using LIGA technology (a high-precision, lithographically defined plating technology) are used to build small flying microhelicopters, which are commercially available from the Institute of Microtechnology in Mainz, Germany, as rather expensive demonstration objects [18.114]. Besides the pure mechanical microrobots, hybrid systems consisting of electromechanical components and living organisms such as cockroaches have also been reported [18.117].

18.7.2 Bio-microrobotics

Biomanipulation entails such operations as positioning, grasping, and injecting material into various locations in cells. Research topics in bio-microrobotics include the autonomous manipulation of single cells or molecules,

the characterization of biomembrane mechanical properties using microrobotic systems with integrated vision and force sensing modules, and more. The objective is to obtain a fundamental understanding of single-cell biological systems and provide characterized mechanical models of biomembranes for deformable cell tracking during biomanipulation and cell injury studies.

Existing biomanipulation techniques can be classified into noncontact manipulation including laser trapping [18.118–121] and electrorotation [18.122–124], and contact manipulation, referred to as mechanical micromanipulation [18.125]. When laser trapping [18.118–121] is used for noncontact biomanipulation, a laser beam is focused through a large-numerical-aperture objective lens, converging to form an optical trap in which the lateral trapping force moves a cell in suspension toward the center of the beam. The longitudinal trapping force moves the cell in the direction of the focal point. The optical trap levitates the cell and holds it in position. Laser traps can work in a well-controlled manner. However, two features make laser trapping techniques undesirable for automated cell injection. The high dissipation of visible light in aqueous solutions requires the use of high-energy light close to the UV spectrum, raising the possibility of damage to the cell. Even though some researchers claim that such concerns could be overcome using wavelengths in the near-infrared (IR) spectrum [18.120], the question as to whether the incident laser beam might induce abnormalities in the cells' genetic material still exists. One alternative to using laser beams is the electrorotation technique. Electric-field-induced rotation of cells was demonstrated by *Mischel* [18.126], *Arnold* [18.127], and *Washizu* [18.124]. This noncontact cell manipulation technique is based on controlling the phase shift and magnitude of electric fields. These fields, appropriately applied, produce a torque on the cell. Different system configurations have been established for cell manipulation based on this principle [18.122, 123], which can achieve high accuracy in cell positioning. However, it lacks a means to hold the cell in place for further manipulation, such as injection, since the magnitude of the electric fields has to be kept low to ensure the viability of cells. The limits of noncontact biomanipulation in the laser trapping and electrorotation techniques make mechanical micromanipulation desirable. The damage caused by laser beams in the laser trapping technique and the lack of a holding mechanism in the electrorotation technique can be overcome by mechanical micromanipulation.

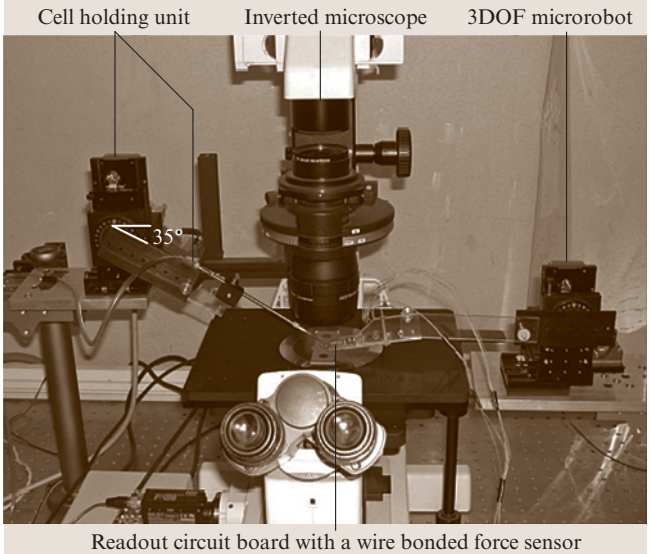

Fig. 18.9 Robotic biomanipulation system with vision and force feedback

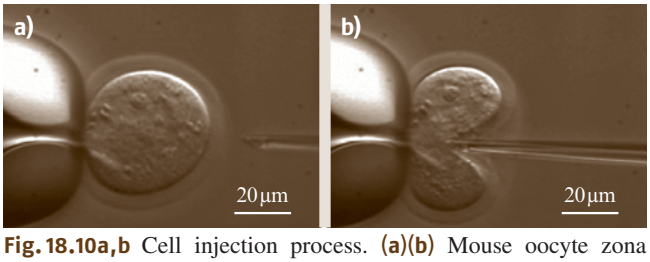

Fig. 18.10a,b Cell injection process. **(a)(b)** Mouse oocyte zona pellucida (ZP)

To improve the low success rate of manual operation, and to eliminate contamination, an autonomous robotic system (shown in Fig. 18.9) has been developed to deposit DNA into one of the two nuclei of a mouse embryo without inducing cell lysis [18.11, 128]. The laboratory's experimental results show that the success rate for the autonomous embryo pronuclei DNA injection is dramatically improved over conventional manual injection methods. The autonomous robotic system features a hybrid controller that combines visual servoing and precision position control, pattern recognition for detecting nuclei, and a precise autofocusing scheme. Figure 18.10 illustrates the injection process.

To realize large-scale injection operations, a MEMS cell holder was fabricated using anodic wafer-bonding techniques. Arrays of holes are aligned on the cell holder, which are used to contain and fix individual cells for

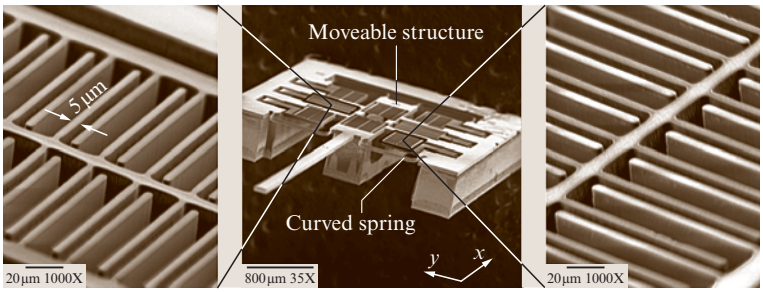

Fig. 18.11 A cellular force sensor with orthogonal comb drives detailed

injection. When well calibrated, the system with the cell holder makes it possible to inject large numbers of cells using position control. The cell injection operation can be conducted in a move–inject–move manner.

A successful injection is determined greatly by injection speed and trajectory, and the forces applied to cells. To further improve the robotic system's performance, a multi-axial MEMS-based capacitive cellular force sensor is being designed and fabricated to provide realtime force feedback to the robotic system. The MEMS cellular force sensor also aids research in biomembrane mechanical property characterization.

MEMS-Based Multi-Axis Capacitive Cellular Force Sensor

The MEMS-based two-axis cellular force sensor [18.129] shown in Fig. 18.11 is capable of resolving normal forces applied to a cell as well as tangential forces generated by improperly aligned cell probes. A high-yield microfabrication process was developed to form the 3-D high-aspect-ratio structure using deep reactive ion etching (DRIE) on silicon-on-insulator (SOI) wafers. The constrained outer frame and the inner movable structure are connected by four curved springs. A load applied to the probe causes the inner structure to move, changing the gap between each pair of interdigitated comb capacitors. Consequently, the total capacitance change resolves the applied force. The interdigitated capacitors are orthogonally configured to make the force sensor capable of resolving forces in both the x- and y-directions. The cellular force sensors used in the experiments are capable of resolving forces up to 25 μN with a resolution of 0.01 μN.

Tip geometry affects the quantitative force measurement results. A standard injection pipette (Cook K-MPIP-1000-5) tip section with a tip diameter of 5 μm is attached to the probe of the cellular force sensors.

The robotic system and high-sensitivity cellular force sensor are also applied to biomembrane mechanical property studies [18.130]. The goal is to obtain a general parameterized model describing cell membrane deformation behavior when an external load is applied. This parameterized model serves two chief purposes. First, in robotic biomanipulation, it allows online parameter recognition so that cell membrane deformation behavior can be predicted. Second, for a thermodynamic model of membrane damage in cell injury and recovery studies, it is important to appreciate the mechanical behavior of the membranes. This allows the interpretation of such reported phenomena as mechanical resistance to cellular volume reduction during dehydration, and its relationship to injury. The establishment of such a biomembrane model will greatly facilitate cell injury studies.

Experiments demonstrate that robotics and MEMS technology can play important roles in biological studies such as automating biomanipulation tasks. Aided by robotics, the integration of vision and force sensing modules, and MEMS design and fabrication techniques, investigations are being conducted in biomembrane mechanical property modeling, deformable cell tracking, and single-cell and biomolecule manipulation.

18.8 Nanorobotics

Nanorobotics represents the next stage in miniaturization for maneuvering nanoscale objects. Nanorobotics is the study of robotics at the nanometer scale, and includes robots that are nanoscale in size, i. e., nanorobots, and large robots capable of manipulating objects that have dimensions in the nanoscale range with nanometer resolution, i. e., nanorobotic manipulators. Robotic manipulation at nanometer scales is a promising tech-

nology for structuring, characterizing, and assembling nanoscale building blocks into NEMS. Combined with recently developed nanofabrication processes, a hybrid approach is realized to build NEMS and other nanorobotic devices from individual carbon nanotubes and SiGe/Si nanocoils. Material science, biotechnology, electronics, and mechanical sensing and actuation will benefit from advances in nanorobotics.

18.8.1 Introduction to Nanomanipulation

Nanomanipulation, or positional and/or force control at the nanometer scale, is a key enabling technology for nanotechnology by filling the gap between top-down and bottom-up strategies, and may lead to the appearance of replication-based molecular assemblers [18.18]. These types of assemblers have been proposed as general-purpose manufacturing devices for building a wide range of useful products as well as copies of themselves (self-replication).

Presently, nanomanipulation can be applied to the scientific exploration of mesoscopic physical phenomena, biology, and the construction of prototype nanodevices. It is a fundamental technology for property characterization of nanomaterials, nanostructures, and nanomechanisms, for the preparation of nanoscale building blocks, and for the assembly of nanodevices such as NEMS.

Nanomanipulation was enabled by the inventions of the STM [18.19], AFMs [18.44], and other types of SPMs. Besides these, optical tweezers (laser trapping) [18.131] and magnetic tweezers [18.132] are also potential nanomanipulators. Nanorobotic manipulators (NRMs) [18.133,134] are characterized by the capability of 3-D positioning, orientation control, independently actuated multiple end-effectors, and independent real-time observation systems, and can be integrated with scanning probe microscopes. NRMs largely extend the complexity of nanomanipulation.

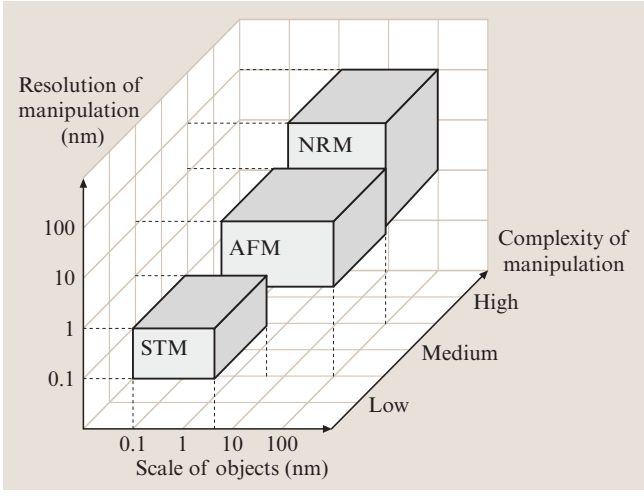

Fig. 18.12 Comparison of nanomanipulators

A concise comparison of STM, AFM, and NRM technology is shown in Fig. 18.12. With its incomparable imaging resolution, an STM can be applied to particles as small as atoms with atomic resolution. However, limited by its 2-D positioning and available strategies for manipulations, standard STMs are ill-suited for complex manipulation and cannot be used in 3-D space. An AFM is another important type of nanomanipulator. Manipulation with an AFM can be done in either contact or dynamic mode. Generally, manipulation with an AFM involves moving an object by touching it with a tip. A typical manipulation starts by imaging a particle in noncontact mode, then removing the tip oscillation voltage and sweeping the tip across the particle in contact with the surface and with the feedback disabled. Mechanical pushing can exert larger forces on objects and, hence, can be applied for the manipulation of relatively larger objects. 1- to 3-D objects can be manipulated on a 2-D substrate. However, the manipulation of individual atoms with an AFM remains a challenge. By separating the imaging and manipulation functions, nanorobotic manipulators can have many more degrees of freedom including rotation for orientation control, and hence can be used for the manipulation of 0-D (symmetric spheres) to 3-D objects in 3-D free space. Limited by the lower resolution of electron microscopes, NRMs are difficult to use for the manipulation of atoms. However, their general robotic capabilities, including 3-D positioning, orientation control, independently actuated multiple endeffectors, separate real-time observation system, and integration with SPMs inside, make NRMs quite promising for complex nanomanipulation.

The first nanomanipulation experiment was performed by *Eigler* and *Schweizer* in 1990 [18.135]. They used an STM and materials at low temperatures (4 K) to position individual xenon atoms on a single-crystal nickel surface with atomic precision. The manipulation enabled them to fabricate rudimentary structures of their own design, atom by atom. The result is the famous set of images showing how 35 atoms were moved to form the three-letter logo *IBM*, demonstrating that matter could indeed be maneuvered atom by atom as *Feynman* suggested [18.1].

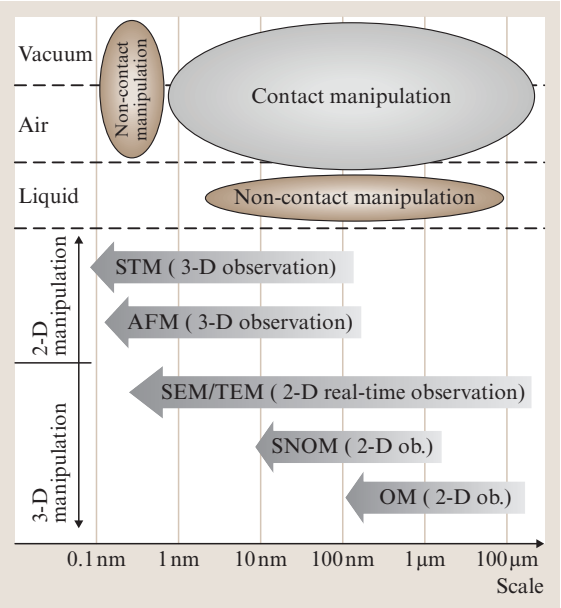

Fig. 18.13 Microscopes, environments, and strategies of nanomanipulation

A nanomanipulation system generally includes nanomanipulators as the positioning device, microscopes as *eyes*, various end-effectors including probes and tweezers among others as its *fingers*, and various types of sensors (force, displacement, tactile, strain, etc.) to facilitate the manipulation and/or to determine the properties of the objects. Key technologies for nanomanipulation include observation, actuation, measurement, system design and fabrication, calibration and control, communication, and the human–machine interface.

Strategies for nanomanipulation are basically determined by the environment – air, liquid or vacuum – which is further decided by the properties and size of the objects and observation methods. Figure 18.13 depicts the microscopes, environments, and strategies of nanomanipulation. In order to observe manipulated objects, STMs can provide sub-Ångström imaging resolution, whereas AFMs can provide atomic resolutions. Both can obtain 3-D surface topology. Because AFMs can be used in an ambient environment, they provide a powerful tool for biomanipulation that may require a liquid environment. The resolution of SEM is limited to about 1 nm, whereas field-emission SEM (FESEM) can achieve higher resolutions. SEM/FESEM can be used for real-time 2-D observation for both the objects and end-effectors of manipulators, and large ultrahigh-vacuum (UHV) sample chambers provide enough space to contain an NRM with many degrees of freedom (DOFs) for 3-D nanomanipulation. However, the 2-D nature of the observation makes positioning along the electron-beam direction difficult. High-resolution transmission electron microscopes (HRTEM) can provide atomic resolution. However, the narrow UHV specimen chamber makes it difficult to incorporate large manipulators. In principle, optical microscopes (OMs) cannot be used for nanoscale (smaller than the wavelength of visible lights) observation because of diffraction limits. Scanning near-field OMs (SNOMs) break this limitation and are promising as a real-time observation device for nanomanipulation, especially for ambient environments. SNOMs can be combined with AFMs, and potentially with NRMs for nanoscale biomanipulation.

Nanomanipulation processes can be broadly classified into three types:

1. lateral noncontact
2. lateral contact
3. vertical manipulation

Generally, lateral noncontact nanomanipulation is mainly applied for atoms and molecules in UHV with an STM or bio-object in liquid using optical or magnetic tweezers. Contact nanomanipulation can be used in almost any environment, generally with an AFM, but is difficult for atomic manipulation. Vertical manipulation can be performed by NRMs. Figure 18.14 shows the processes of the three basic strategies.

Motion of the lateral noncontact manipulation processes is shown in Fig. 18.14a. Applicable effects [18.136] able to cause the motion include long-range van der Waals (vdW) forces (attractive) generated by the proximity of the tip to the sample [18.137], electric-field-induced fields by the voltage bias between the tip and the sample [18.138,139], tunneling current local heating or inelastic tunneling vibration [18.140,141]. With these methods, some nanodevices and molecules have been assembled [18.142,143]. Laser trapping (optical tweezers) and magnetic tweezers are possible for noncontact manipulation of nanoscale biosamples, e.g., DNA [18.144,145].

Noncontact manipulation combined with STMs has revealed many possible strategies for manipulating atoms and molecules. However, for the manipulation of carbon nanotubes (CNTs) no examples have been demonstrated.

Pushing or pulling nanometer objects on a surface with an AFM is a typical manipulation using this method as shown in Fig. 18.14b. Early work showed

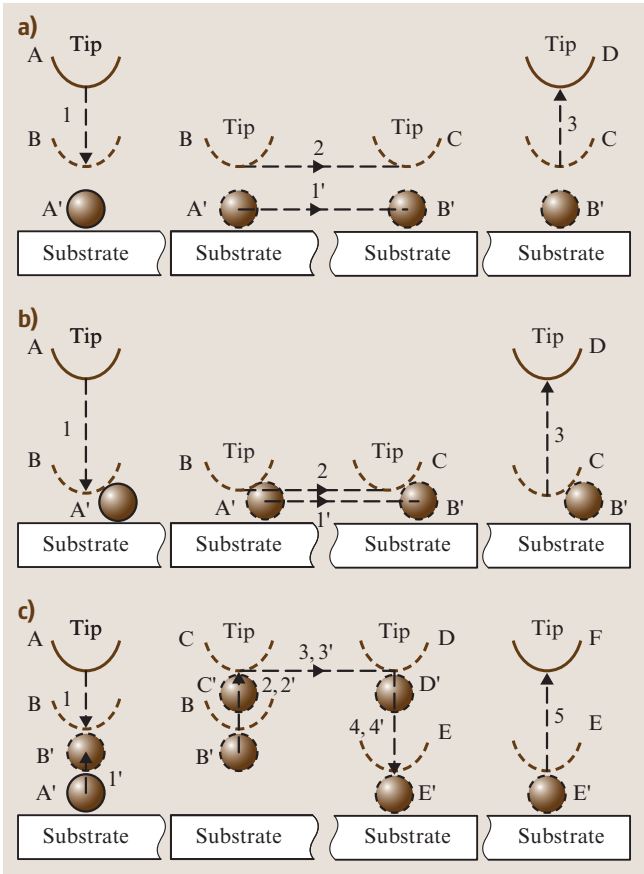

Fig. 18.14a–c Basic strategies of nanomanipulation. In the figure, A, B, C, ... represent the positions of end-effector (e.g., a tip); A′, B′, C′, ... the positions of objects; 1, 2, 3, ... the motions of end-effector; and 1′, 2′, 3′, ... the motions of objects. Tweezers can be used in pick-and-place to facilitate the picking-up, but are generally not necessarily helpful for placing. **(a)** Lateral noncontact nanomanipulation (sliding). **(b)** Lateral contact nanomanipulation (pushing/pulling). **(c)** Vertical nanomanipulation (picking and placing)

the effectiveness of this method for the manipulation of nanoparticles [18.146–150]. This method has also been shown in nanoconstruction [18.151] and biomanipulation [18.152]. A virtual-reality interface facilitates such manipulation [18.153–155] and may create an opportunity for other types of manipulation. This technique has been used in the manipulation of nanotubes on a surface, and some examples will be introduced later in this chapter.

The pick-and-place task as shown in Fig. 18.14c is especially significant for 3-D nanomanipulation since its main purpose is to assemble prefabricated building blocks into devices. The main difficulty is in achieving sufficient control of the interaction between the tool and object and between the object and the substrate. Two strategies have been presented for micromanipulation [18.156] and have also proven to be effective for nanomanipulation [18.134]. One strategy is to apply a dielectrophoretic force between a tool and an object as a controllable additional external force by applying a bias between the tool and the substrate on which the object is placed. Another strategy is to modify the van der Waals and other intermolecular and surface forces between the object and the substrate. For the former, an AFM cantilever is ideal as one electrode to generate a nonuniform electrical field between the cantilever and the substrate.

18.8.2 Nanorobotic Manipulation Systems

Nanorobotic manipulators are the core components of nanorobotic manipulation systems. The basic requirements for a nanorobotic manipulation system for 3-D manipulation include nanoscale positioning resolution, a relative large working space, enough DOFs including rotational ones for 3-D positioning and orientation control of the end-effectors, and usually multiple end effectors for complex operations.

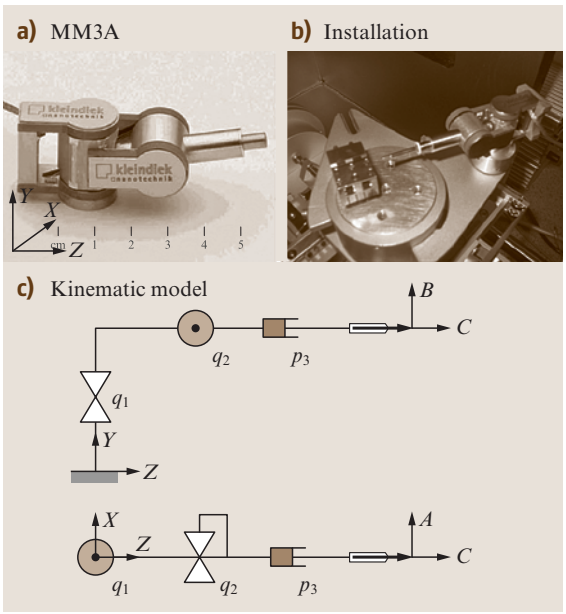

Fig. 18.15 **(a)** Nanomanipulator (MM3A)^{TM} from Kleindiek **(b)** inside an SEM

Table 18.4 Specifications of MM3A

Item	Specification
Operating range q_1 and q_2	240°
Operating range Z	12 mm
Resolution A (horiz.)	10^{-7} rad (5 nm)
Resolution B (vert.)	10^{-7} rad (3.5 nm)
Resolution C (linear)	0.25 nm
Fine (scan) range A	20 μm
Fine (scan) range B	15 μm
Fine (scan) range C	1 μm
Speed A, B	10 mm/s
Speed C	2 mm/s

A commercially available nanomanipulator (MM3A^{TM} from Kleindiek) installed inside an SEM (Carl Zeiss DSM962) is shown in Fig. 18.15. The manipulator has three degrees of freedom, and nanometer- to subnanometer-scale resolution (Table 18.4). Calculations show that when moving/scanning in the A/B direction at joint q_1/q_2, the additional linear motion in C is very small. For example, when the arm length is 50 mm, the additional motion in the C direction is only 0.25 nm to 1 nm when moving 5–10 μm; in the A direction; these errors can be ignored or compensated with an additional motion of the prismatic joint p_3, which has a 0.25 nm resolution.

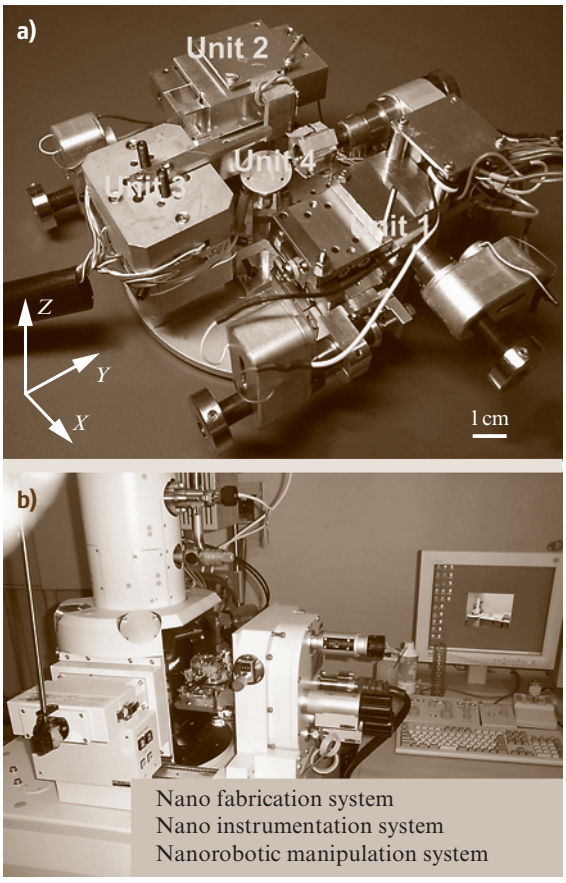

Fig. 18.16a,b Nanorobotic system. **(a)** Nanorobotic manipulators. **(b)** System setup

Figure 18.16a shows a nanorobotic manipulation system that has 16 DOFs in total and can be equipped with three or four AFM cantilevers as end-effectors for both manipulation and measurement. The positioning resolution is sub-nanometer and strokes are on the order of centimeters. The manipulation system is not only for nanomanipulation, but also for nanoassembly, nanoinstrumentation, and nanofabrication. Four-probe semiconductor measurements are perhaps the most complex manipulation that this system can perform, because it is necessary to actuate four probes independently by using four manipulators. With the advancement of nanotechnology, one could shrink the size of nanomanipulators and insert more DOFs inside the limited vacuum chamber of a microscope, and perhaps the molecular version of manipulators such as that dreamed of by Drexler could be realized [18.18].

For the construction of multi-walled carbon nanotube (MWNT)-based nanostructures, manipulators position and orient nanotubes for the fabrication of nanotube probes and emitters, for performing nanosoldering with electron-beam-induced deposition (EBID) [18.157], for the property characterization of single nanotubes for selection purposes and for characterizing junctions to test connection strength.

A nanolaboratory is shown in Fig. 18.16b. The nanolaboratory integrates a nanorobotic manipulation system with a nanoanalytical system and a nanofabrication system, and can be applied for manipulating nanomaterials, fabricating nanoscale building blocks, assembling nanodevices, and for in situ analysis of the properties of such materials, building blocks, and devices. Nanorobotic manipulation within the nanolaboratory has opened a new path for constructing nanosystems in 3-D space, and will create opportunities for new nanoinstrumentation and nanofabrication processes.

18.8.3 Nanorobotic Assembly

Nanomanipulation is a promising strategy for nanoassembly. Key techniques for nanoassembly include the structuring and characterization of nanoscale building

blocks, the positioning and orientation control of the building blocks with nanoscale resolution, and effective connection techniques. Nanorobotic manipulation, which is characterized by multiple DOFs with both position and orientation controls, independently actuated multiprobes, and a real-time observation system, have been shown effective for assembling nanotube-based devices in 3-D space.

The well-defined geometries, exceptional mechanical properties, and extraordinary electric characteristics, among other outstanding physical properties of CNTs [18.158] qualify them for many potential applications, especially in nanoelectronics [18.159], NEMS, and other nanodevices [18.160]. For NEMS, some of the most important characteristics of nanotubes include their nanometer diameter, large aspect ratio (10-1000), TPa-scale Young's modulus [18.161–163], excellent elasticity [18.133], ultralow interlayer friction, excellent capability for field emission, various electric conductivities [18.164], high thermal conductivity [18.165], high current-carrying capability with essentially no heating [18.166], sensitivity of conductance to various physical or chemical changes, and charge-induced bond-length change.

Helical 3-D nanostructures, or nanocoils, have been synthesized from various materials, including helical carbon nanotubes [18.167] and zinc oxide nanobelts [18.168]. A new method of creating structures with nanoscale dimensions has recently been presented [18.169] and can be fabricated in a controllable way [18.170, 171]. The structures are created through a top-down fabrication process in which a strained nanometer-thick heteroepitaxial bilayer curls up to form 3-D structures with nanoscale features. Helical geometries and tubes with diameters between 10 nm and 10 μm have been achieved. Because of their interesting morphology, mechanical, electrical, and electromagnetic properties, potential applications of these nanostructures in NEMS include nanosprings [18.172], electromechanical sensors [18.173], magnetic field detectors, chemical or biological sensors, generators of magnetic beams, inductors, actuators, and high-performance electromagnetic wave absorbers.

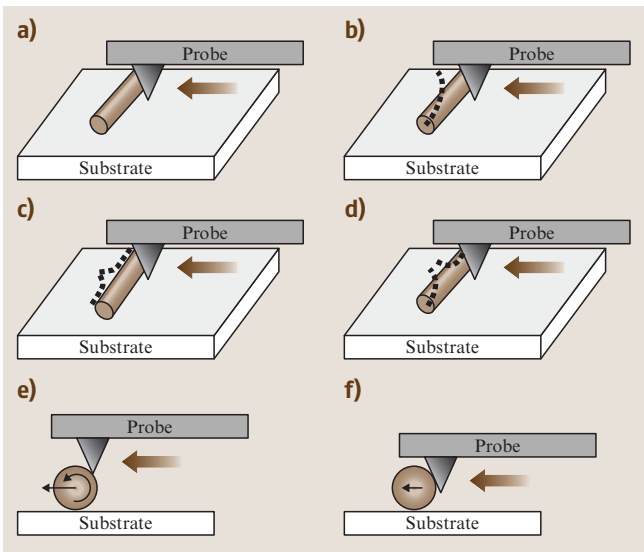

Fig. 18.17a–f Two-dimensional manipulation of CNTs. Starting from the original state shown in **(a)**, pushing the tube at different site with different force may cause the tube to deform as in **(b)** and **(c)**, to break as in **(d)**, or to move as in **(e)** and **(f)**. **(a)**Original state. **(b)**Bending. **(c)**Kinking. **(d)**Breaking. **(e)**Rolling. **(f)**Sliding

NEMS based on individual carbon nanotubes and nanocoils are of increasing interest, indicating that capabilities for incorporating these individual building blocks at specific locations on a device must be developed. Random spreading [18.174], direct growth [18.175], self-assembly [18.176], dielectrophoretic assembly [18.177, 178], and nanomanipulation [18.179] have been demonstrated for positioning as-grown nanotubes on electrodes for the construction of these devices. However, for nanotube-based structures, nanorobotic assembly is still the only technique capable of in situ structuring, characterization, and assembly. Because the as-fabricated nanocoils are not free-standing from their substrate, nanorobotic assembly is virtually the only way to incorporate them into devices at present.

Nanorobotic Assembly of Carbon Nanotubes

Nanotube manipulation in two dimensions on a surface was first performed with an AFM by contact pushing on a substrate. Figure 18.17 shows the typical methods for 2-D pushing. Although similar to that shown in Fig. 18.14b, the same manipulation caused various results because nanotubes cannot be regarded as a 0-D point. The first demonstration was given by *Lieber* and coworkers for measuring the mechanical properties of a nanotube [18.180]. They adopt the method shown in Fig. 18.17b, i. e., to bend a nanotube by pushing one end of it and fixing the other end. The same strategy was used for the investigation of the behavior of nanotubes under large strain [18.181]. *Dekker* and coworkers applied the strategies shown in Fig. 18.17c,d to obtain a kinked junction and crossed nanotubes [18.182]. *Avouris* and coworkers combined this technique with an inverse process, namely straightening by pushing

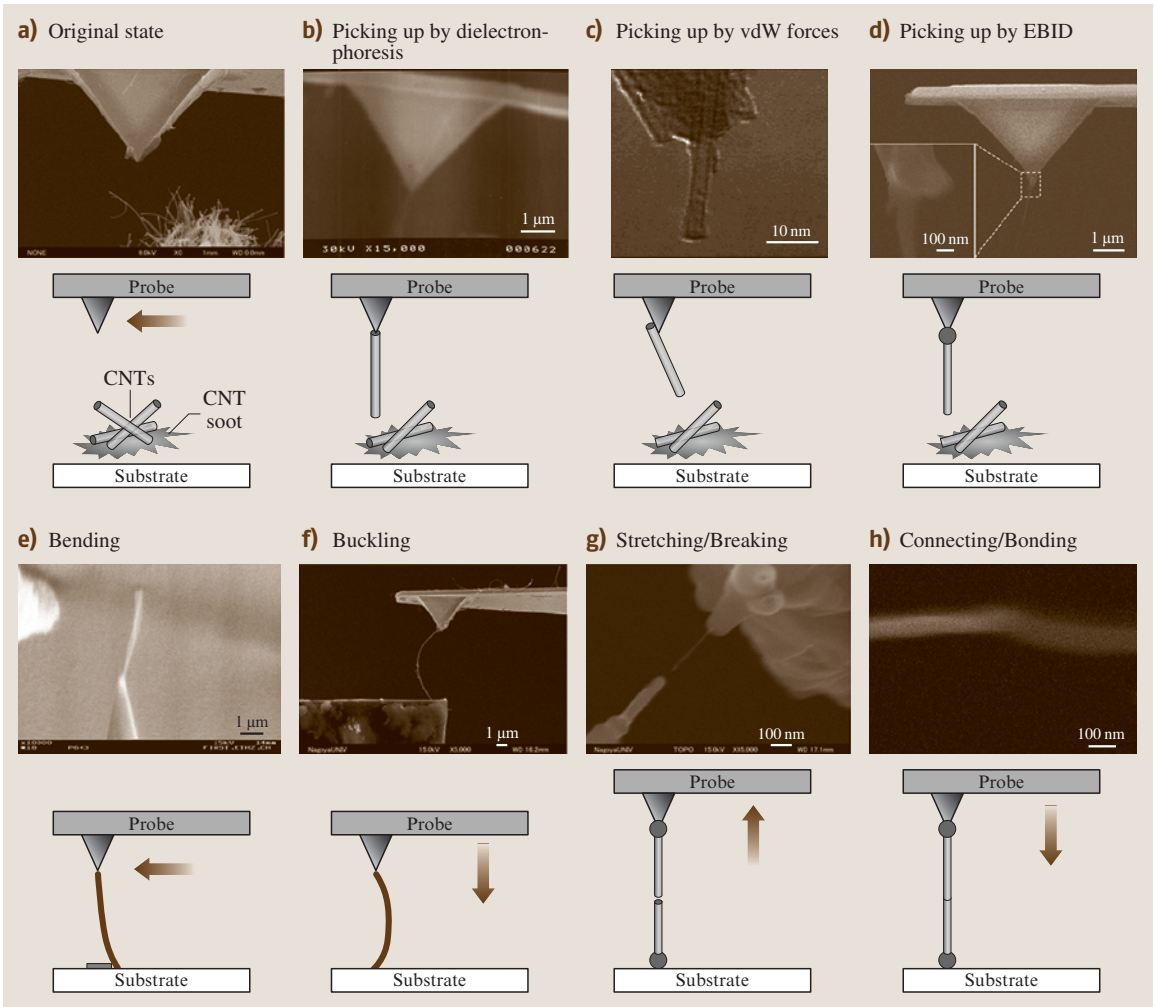

Fig. 18.18a–h Nanorobotic manipulation of CNTs. The basic technique is to pick up an individual tube from CNT soot (as in **(a)**) or from an oriented array; **(b)** shows a free-standing nanotube picked up by dielectrophoresis generated by a nonuniform electric field between the probe and substrate, **(c)** (after [18.188]) and **(d)** show the same manipulation by contacting a tube with the probe surface or fixing (e.g., with EBID) a tube to the tip (inset shows the EBID deposit). Vertical manipulation of nanotubes includes bending **(e)**, buckling **(f)**, stretching/breaking **(g)**, and connecting/bonding **(h)**. All examples with the exception of **(c)** are from the authors' work

along a bent tube, and realized the translation of the tube to another location [18.183] and between two electrodes to measure the conductivity [18.184]. This technique was also used to place a tube on another tube to form a single-electron transistor (SET) with a cross-junction of nanotubes [18.185]. Pushing-induced breaking (Fig. 18.17d) has also been demonstrated for a nanotube [18.183]. The simple assembly of two bent tubes and a straight one formed a Greek letter θ. To investigate the dynamics of rolling at the atomic level, rolling and sliding of a nanotube (as shown in Fig. 18.17e,f) are performed on graphite surfaces using an AFM [18.186]. Besides pushing and pulling, another important process is indentation. By indenting a surface, mechanical property characterization [18.187] and data storage [18.188] can be realized.

Manipulation of CNTs in 3-D space is important for assembling CNTs into structures and devices. Basic

techniques for the nanorobotic manipulation of carbon nanotubes are shown in Fig. 18.18 [18.189]. These serve as the basis for handling, structuring, characterizing, and assembling NEMS.

The basic procedure is to pick up a single tube from nanotube soot (Fig. 18.18a). This has been shown first by using dielectrophoresis [18.134] through nanorobotic manipulation (Fig. 18.18b). By applying a bias between a sharp tip and a plane substrate, a nonuniform electric field can be generated between the tip and the substrate with the strongest field near the tip. This field can cause a tube to orient along the field or further *jump* to the tip by electrophoresis or dielectrophoresis (determined by the conductivity of objective tubes). Removing the bias, the tube can be placed at other locations at will. This method can be used for free-standing tubes on nanotube soot or on a rough surface on which surface van der Waals forces are generally weak. A tube strongly rooted in CNT soot or lying on a flat surface cannot be picked up in this way. The interaction between a tube and the atomic flat surface of AFM cantilever tip has been shown to be strong enough for picking up a tube onto the tip [18.190] (Fig. 18.18c). By using EBID, it is possible to pick up and fix a nanotube onto a probe [18.191] (Fig. 18.18d). For handling a tube, weak connection between the tube and the probe is desired.

Bending and buckling a CNT as shown in Fig. 18.18e,f are important for in situ property characterization of a nanotube[18.192], which is a simple way to obtain the Young's modulus of a nanotube without damaging the tube (if performed within its elastic range) and hence can be used for the selection of a tube with desired properties. By buckling an MWNT over its elastic limit, a kinked structure can be obtained [18.193]. To obtain any desired angle for a kinked junction it is possible to fix the shape of a buckled nanotube within its elastic limit by using EBID [18.193]. For a CNT, the maximum angular displacement will appear at the fixed left end under pure bending or at the middle point under pure buckling. A combination of these two kinds of loads will achieve a controllable position of the kinked point and a desired kink angle. If the deformation is within the elastic limit of the nanotube, it will recover as the load is released. To avoid this, EBID can be applied at the kinked point to fix the shape.

Stretching a nanotube between two probes or a probe and a substrate has generated several interesting results (Fig. 18.18g). The first demonstration of 3-D nanomanipulation of nanotubes took this as an example to show the breaking mechanism and to measure the tensile strength of CNTs[18.133]. By breaking an MWNT in a controlled manner, interesting nanodevices have been fabricated. This technique – destructive fabrication – has been presented to get sharpened and layered structures of nanotubes, and to improve the length control of a nanotube [18.193]. Typically, a layered and a sharpened structure can be obtained from this process, similar to that achieved from electric pulses [18.194]. Bearing motion has also been observed in an incompletely broken MWNT [18.193]. The interlayer friction has been shown to be very small [18.195, 196].

The reverse process, namely the connection of broken tubes (Fig. 18.18h), has been demonstrated recently, and the mechanism is revealed as rebonding of unclosed dangling bonds at the ends of broken tubes [18.197]. Based on this interesting phenomenon, mechanochemical nanorobotic assembly has been performed [18.197].

Assembly of nanotubes is a fundamental technology for enabling nanodevices. The most important tasks include the connection of nanotubes and placing of nanotubes onto electrodes. Pure nanotube circuits [18.198] created by interconnecting nanotubes of different diameters and chirality could lead to further size reductions in devices. Nanotube intermolecular and intramolecular junctions are basic elements for such systems [18.199]. Room-temperature (RT) single-electron transistors (SETs) [18.200] have been shown with a short ($\approx 20\,\mathrm{nm}$) nanotube section that is created by inducing local barriers into the tube with an AFM, and Coulomb charging has been observed. With a cross-junction of two single-walled carbon nanotubes (SWNTs) (semiconducting/metallic), three- and four-terminal electronic devices have been made [18.201]. A suspended cross-junction can function as an electromechanical nonvolatile memory [18.202].

Although some kinds of junctions have been synthesized with chemical methods, there is no evidence yet showing that a self-assembly-based approach can provide more complex structures. SPMs were also used to fabricate junctions, but they are limited to a 2-D plane. We have presented 3-D nanorobotic manipulation-based nanoassembly, which is a promising strategy both for the fabrication of nanotube junctions and for the construction of more complex nanodevices with such junctions as well.

Nanotube junctions can be classified into different types by the kinds of components (SWNTs or MWNTs), geometric configurations (V kink, I, X cross, T, Y branch, and 3-D junctions) conductivity (metallic or semiconducting), and connection methods [intermolecular (connected with van der Waals force, EBID, etc.) or intramolecular (connected with chemical bonds) junc-

tions]. Here we show the fabrication of several kinds of MWNT junctions by emphasizing the connection methods. These methods will also be effective for SWNT junctions. Figure 18.19 shows CNT junctions constructed by connecting with van der Waals forces (a), joining by electron-beam-induced deposition (b), and bonding through mechanochemistry (c).

Figure 18.19a shows a T-junction connected with van der Waals forces, which is fabricated by positioning the tip of an MWNT onto another MWNT until they form a bond. The contact is checked by measuring the shear connection force.

EBID provides a soldering method to obtain stronger nanotube junctions than those connected through van der Waals forces. Hence, if the strength of nanostructures is emphasized, EBID can be applied. Figure 18.19b shows an MWNT junction connected through EBID, in which the upper MWNT is a single one with 20 nm in diameter and the lower one is a bundle of MWNTs with an extruded single CNT with ∅30 nm. The development of conventional EBID has been limited by the expensive electron filament used and low productivity. We have presented a parallel EBID system by using CNTs as emitters because of their excellent field-emission properties [18.203]. The feasibility of parallel EBID is presented. It is a promising strategy for large-scale fabrications of nanotube junctions. As in its macroscale counterpart, welding, EBID works by adding materials to obtain stronger connections, but in some cases, the added material might influence normal functions for nanosystems. So, EBID is mainly applied to nanostructures rather than nanomechanisms.

To construct stronger junctions without adding additional materials, mechanochemical nanorobotic assembly is an important strategy. Mechanochemical nanorobotic assembly is based on solid-phase chemical reactions, or mechanosynthesis, which is defined as chemical synthesis controlled by mechanical systems operating with atomic-scale precision, enabling direct positional selection of reaction sites [18.18]. By picking up atoms with dangling bonds rather than natural atoms only, it is easier to form primary bonds, which provides a simple but strong connection. Destructive fabrication provides a way to form dangling bonds at the ends of broken tubes. Some of the dangling bonds may close with neighboring atoms, but generally a few bonds will remain dangling. A nanotube with dangling bonds at its end will bind more easily to another to form intramolecular junctions. Figure 18.19c shows such a junction.

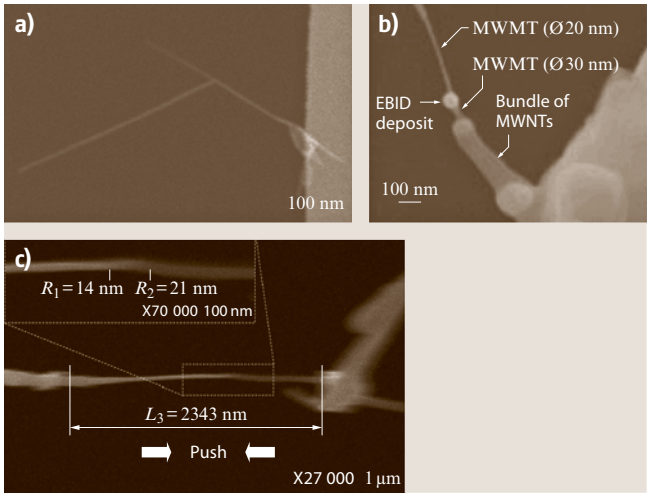

Fig. 18.19a–c MWNT junctions. **(a)** MWNTs connected with van der Waals forces. **(b)** MWNTs joined with EBID. **(c)** MWNTs bonded with a mechanochemical reaction

Three-dimensional nanorobotic manipulation has opened a new route for the structuring and assembly of nanotubes into nanodevices. However, at present nanomanipulation is still performed in a serial manner with master–slave control, which is not a large-scale production-oriented technique. Nevertheless, with advances in the exploration of mesoscopic physics, better control on the synthesis of nanotubes, more accurate actuators, and effective tools for manipulation, high-speed and automatic nanoassembly will be possible. Another approach might be parallel assembly by positioning building blocks with an array of probes [18.204] and joining them together simultaneously, e.g., with the parallel EBID [18.191] we presented. Further steps might progress towards exponential assembly [18.205], and in the far future to self-replicating assembly [18.18].

Nanorobotic Assembly of Nanocoils

The construction of nanocoil-based NEMS involves the assembly of as-grown or as-fabricated nanocoils, which is a significant challenge from a fabrication standpoint. Focusing on the unique aspects of manipulating nanocoils due to their helical geometry, high elasticity, single-end fixation, and strong adhesion of the coils to the substrate from wet etching, a series of new processes has been presented using a manipulator (MM3A, Kleindiek) installed in an SEM (Zeiss DSM962). As-fabricated SiGe/Si bilayer nanocoils (thickness 20 nm without Cr layer or 41 nm with Cr layer; diameter $D = 3.4\,\mu m$) are manipulated. Special tools have been

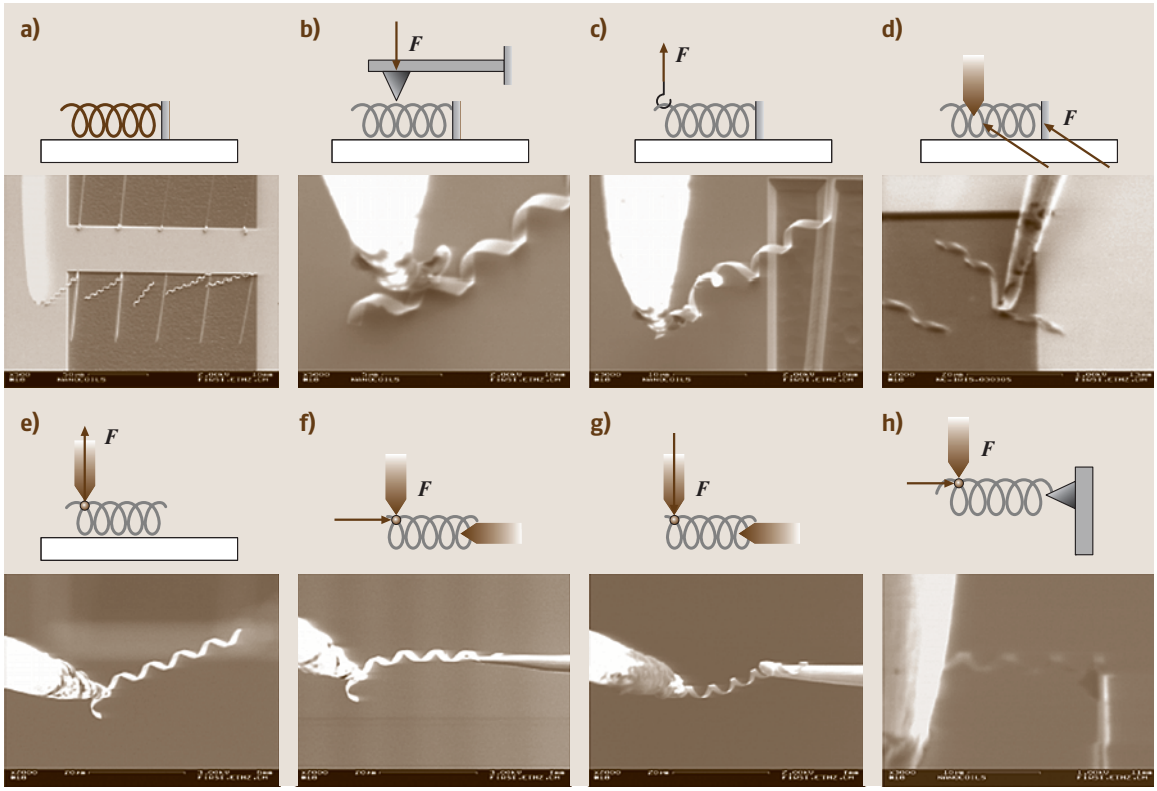

Fig. 18.20a–h Nanorobotic manipulation of nanocoils **(a)** original state, **(b)** compressing/releasing, **(c)** hooking, **(d)** lateral pushing/breaking, **(e)** picking, **(f)** placing/inserting, **(g)** bending, and **(h)** pushing and pulling

fabricated including a nanohook prepared by controlled *tip-crashing* of a commercially available tungsten sharp probe (Picoprobe T-4-10–1 mm and T-4-10) onto a substrate, and a *sticky* probe prepared by tip dipping into a double-sided SEM silver conductive tape (Ted Pella, Inc.). As shown in Fig. 18.20, experiments demonstrate that nanocoils can be released from a chip by lateral pushing, picked up with a nanohook or a *sticky* probe, and placed between the probe/hook and another probe or an AFM cantilever (Nano-probe, NP-S). Axial pulling/pushing, radial compressing/releasing, and bending/buckling have also been demonstrated. These processes have shown the effectiveness of manipulation for the characterization of coil-shaped nanostructures and their assembly for NEMS, which have been otherwise unavailable.

Configurations of nanodevices based on individual nanocoils are shown in Fig. 18.21. Cantilevered nanocoils as shown in Fig. 18.21a can serve as nanosprings. Nanoelectromagnets, chemical sensors, and nanoinductors involve nanocoils bridged between two electrodes as shown in Fig. 18.21b. Electromechanical sensors can use a similar configuration but with one end connected to a moveable electrode as shown in Fig. 18.21c. Mechanical stiffness and electric conductivity are fundamental properties for these devices that must be further investigated.

As shown in Fig. 18.20h, axial pulling is used to measure the stiffness of a nanocoil. A series of SEM images are analyzed to extract the AFM tip displacement and the nanospring deformation, i. e., the relative displacement of the probe from the AFM tip. From this displacement data and the known stiffness of the AFM cantilever, the tensile force acting on the nanospring versus the nanospring deformation was plotted. The deformation of the nanospring was measured relative to the first measurement point. This was necessary because the proper attachment of the nanospring to the AFM cantilever must be verified. Afterwards, it was not possible to return to the point of zero deformation. Instead, the experimental data as presented in Fig. 18.21d has been shifted such that with the calculated linear elastic spring

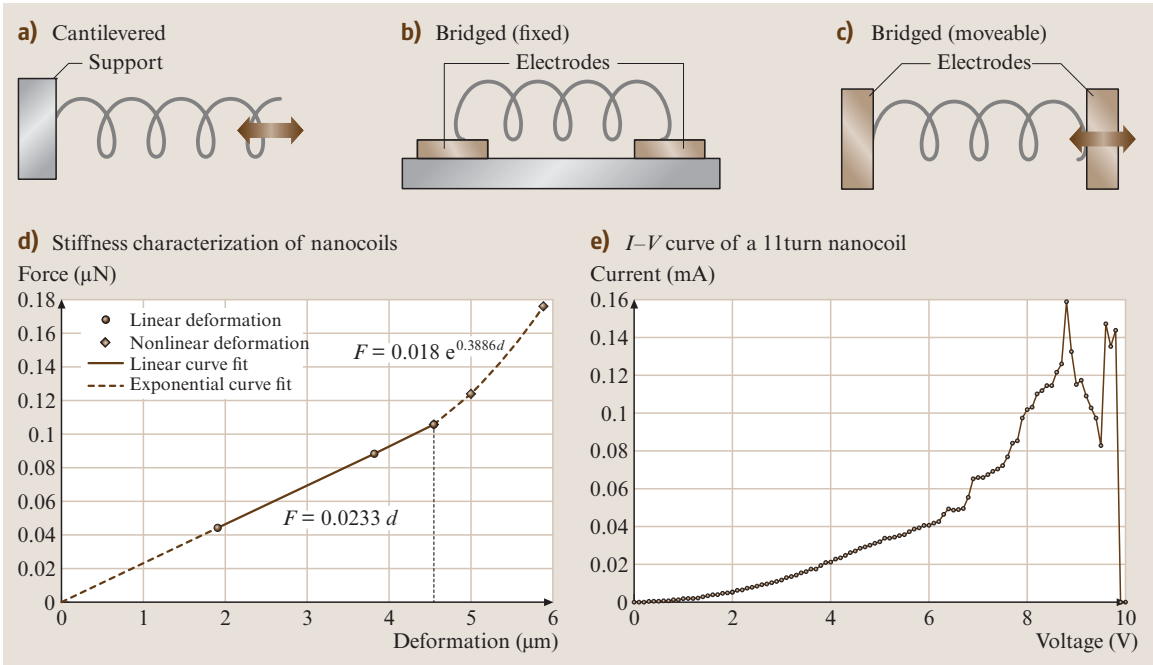

Fig. 18.21a–e Nanocoil-based devices. Cantilevered nanocoils **(a)** can serve as nanosprings. Nanoelectromagnets, chemical sensors, and nanoinductors involve nanocoils bridged between two electrodes **(b)**. Electromechanical sensors can use a similar configuration but with one end connected to a moveable electrode **(c)**. Mechanical stiffness **(d)** and electric conductivity **(e)** are basic properties of interest for these devices

stiffness the line begins at zero force and zero deformation. From Fig. 18.21d, the stiffness of the spring was estimated to be 0.0233 N/m. The linear elastic region of the nanospring extends to a deformation of 4.5 μm. An exponential approximation was fitted to the nonlinear region. When the applied force reached 0.176 μN, the attachment between the nanospring and the AFM cantilever broke. Finite-element simulation (ANSYS 9.0) was used to validate the experimental data [18.173]. Since the exact region of attachment cannot be identified from the SEM images, simulations were conducted for 4, 4.5, and 5 turns to estimate the possible range according to the apparent number of turns of the nanospring. The nanosprings in the simulations were fixed at one end and had an axial load of 0.106 μN applied at the other end. The simulation results for the spring with four turns yield a stiffness of 0.0302 N/m; for the nanospring with 5 turns it is 0.0191 N/m. The measured stiffness falls within this range with 22.0% above the minimum value and 22.8% below the maximum value, and very close to the stiffness of a 4.5-turn nanospring, which has a stiffness of 0.0230 N/m according to the simulation.

Figure 18.21e shows the results from electrical characterization experiments on a nanospring with 11 turns using the configuration shown in Fig. 18.20g. The *I–V* curve is nonlinear, which may be caused by the resistance change of the semiconductive bilayer due to ohmic heating. Another possible reason is the decrease in contact resistance caused by thermal stress. The maximum current was found to be 0.159 mA under an 8.8 V bias. Higher voltage causes the nanospring to *blow off*. From the fast scanning screen of the SEM, an extension of the nanospring on probes was observed around the peak current so that the current does not drop abruptly. At 9.4 V, the extended nanospring is broken down, causing an abrupt drop in the *I–V* curve.

From fabrication and characterization results, the helical nanostructures appear to be suitable to function as inductors. They would allow further miniaturization compared to state-of-the-art microinductors. For this purpose, higher doping of the bilayer and an additional metal layer would result in the required conductance. Conductance, inductance, and quality factor can be further improved if, after curling up, additional metal is electroplated onto the helical structures. Moreover,

a semiconductive helical structure, when functionalized with binding molecules, can be used for chemical sensing under the same principle as demonstrated with other types of nanostructures. With bilayers in the range of a few monolayers, the resulting structures would exhibit very high surface-to-volume ratio with the whole surface exposed to an incoming analyst.

18.8.4 Nanorobotic Devices

Nanorobotic devices involve tools, sensors, and actuators at the nanometer scale. Shrinking device size makes it possible to manipulate nanosized objects with nanosized tools, measure mass in femtogram ranges, sense force at piconewton scales, and induce GHz motion, among other amazing advancements.

Top-down and bottom-up strategies for manufacturing such nanodevices have been independently investigated by a variety of researchers. Top-down strategies are based on nanofabrication and include technologies such as nanolithography, nanoimprinting, and chemical etching. Presently, these are 2-D fabrication processes with relatively low resolution. Bottom-up strategies are assembly-based techniques. At present, these strategies include such techniques as self-assembly, dip-pen lithography, and directed self-assembly. These techniques can generate regular nanopatterns at large scales. With the ability to position and orient nanoscale objects, nanorobotic manipulation is an enabling technology for structuring, characterizing and assembling many types of nanosystems [18.189]. By combining bottom-up and top-down processes, a hybrid nanorobotic approach based on nanorobotic manipulation provides a third way to fabricate NEMS by structuring as-grown nanomaterials or nanostructures. This new nanomanufacturing technique can be used

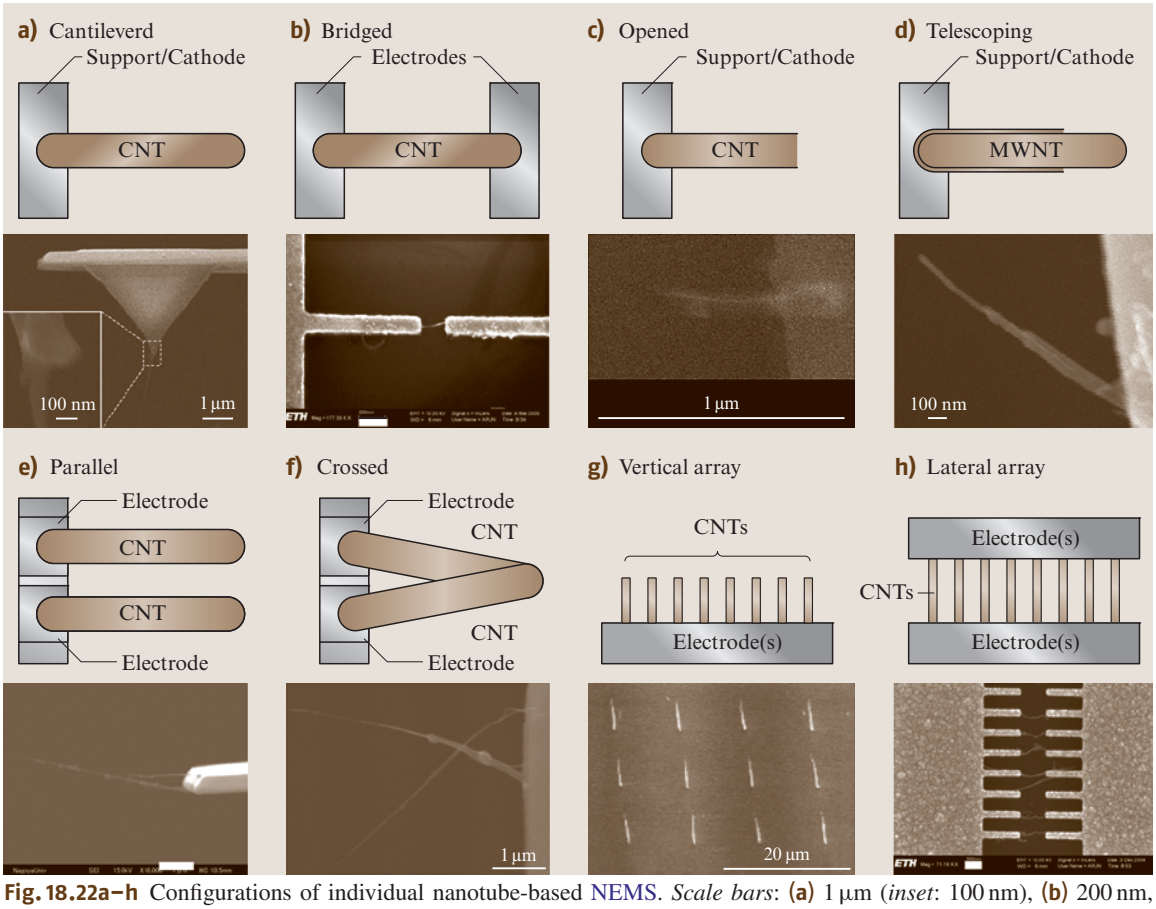

Fig. 18.22a–h Configurations of individual nanotube-based NEMS. *Scale bars*: **(a)** 1 µm (*inset*: 100 nm), **(b)** 200 nm, **(c)** 1 µm, **(d)** 100 nm, **(e)** and **(f)** 1 µm, **(g)** 20 µm, and **(h)** 300 nm. All examples are from the authors' work

to create complex 3-D nanodevices with such building blocks. Nanomaterial science, bio-nanotechnology, and nanoelectronics will also benefit from advances in nanorobotic assembly.

The configurations of nanotools, sensors, and actuators based on individual nanotubes that have been experimentally demonstrated are summarized as shown in Fig. 18.22.

For detecting deep and narrow features on a surface, cantilevered nanotubes (Fig. 18.22a, [18.191]) have been demonstrated as probe tips for an AFM [18.206], a STM, and other types of SPM. Nanotubes provide ultrasmall diameters, ultralarge aspect ratios, and excellent mechanical properties. Manual assembly, and direct growth [18.207] have proven effective for their construction. Cantilevered nanotubes have also been demonstrated as probes for the measurement of ultrasmall physical quantities, such as femtogram masses [18.162], piconewton-order force sensors, and mass flow sensors [18.189] on the basis of their static deflections or change of resonant frequencies detected within an electron microscope. Deflections cannot be measured from micrographs in real time, which limits the application of this kind of sensor. Interelectrode distance changes cause emission current variation of a nanotube emitter and may serve as a candidate to replace microscope images. Bridged individual nanotubes (Fig. 18.22b, [18.177]) have been the basis for electric characterization. Opened nanotubes (Fig. 18.22c, [18.208]) can serve as atomic or molecular containers, thermometers [18.209], or spot welders [18.210]. The electrostatic deflection of a nanotube has been used to construct a relay [18.211]. A new family of nanotube actuators can be constructed by taking advantage of the ultralow interlayer friction of a multiwalled nanotubes. Linear bearings based on telescoping nanotubes and a microactuator with a nanotube as a rotation bearing have been demonstrated [18.195, 212], and batch fabrication has been realized based on dielectrophoretically assembled arrays [18.213]. A preliminary experiment on a promising nanotube linear motor with field-emission current serving as position feedback has been shown with nanorobotic manipulation (Fig. 18.22d, [18.208]). Cantilevered dual nanotubes have been demonstrated as nanotweezers [18.214] and nanoscissors (Fig. 18.22e) [18.179] by manual and nanorobotic assembly, respectively. Based on electric resistance change under different temperatures, nanotube thermal probes (Fig. 18.22f) have been demonstrated for measuring the temperature at precise locations. These thermal probes are more advantageous than nanotube-based thermometers because the latter require TEM imaging. The integration of the aforementioned devices can be realized using the configurations shown in Fig. 18.22g,h [18.177]. The arrays of individual nanotubes can also be used to fabricate nanosensors, such as position encoders [18.215].

Nanotube-based NEMS remains a rich research field with a large number of open problems. New materials such as nanowires, nanobelts, and polymer at the nanoscale will enable a new family of sensors and actuators for the detection and actuation of ultrasmall quantities or objects with ultrahigh precision and frequencies. Through random spreading, direct growth, optical tweezers, and nanorobotic manipulation, prototypes have been demonstrated. However, for integration into NEMS, self-assembly processes will become increasingly important. Among them, we believe that dielectrophoretic nanoassembly will play a significant role for large-scale production of regular 2-D structures.

18.9 Conclusions

Despite the claims of many *futurists*, such as Isaac *Asimov*'s legendary submarine Proteus inside the human body [18.216] and *Robert A. Freitas's* nanomedical robots [18.217], the form that micro/nanorobots of the future will take and the tasks they will actually perform remain unclear. However, it is clear that technology is progressing towards the construction of intelligent sensors, actuators, and systems on small scales. These will serve as both the tools to be used for fabricating future micro/nanorobots as well as the components from which these robots may be developed. Shrinking device size to these dimensions presents many fascinating opportunities such as manipulating nano-objects with nanotools, measuring mass in femtogram ranges, sensing forces at piconewton scales, and inducing GHz motion, among other new possibilities waiting to be discovered. These capabilities will, of course, drive the tasks that future micro/nanorobots constructed by and with MEMS/NEMS will perform.

References

18.1 R.P. Feynman: There's plenty of room at the bottom, Caltech Eng. Sci. **23**, 22–36 (1960)

18.2 R.S. Muller: Microdynamics, Sens. Actuat. A **21–23**, 1–8 (1990)

18.3 A.M. Flynn, R.A. Brooks, W.M. Wells, III, D.S. Barrett: The world's largest one cubic inch robot, Proc. of IEEE 2nd Int. Workshop on Micro Electro Mechanical Systems (IEEE, Piscataway 1989) pp. 98–101

18.4 W. Trimmer, R. Jebens: Actuators for micro robots, Proc. of the 1989 IEEE Int. Conf. on Robotics and Automation (IEEE, Piscataway 1989) pp. 1547–1552

18.5 S. Fatikow, U. Rembold: An automated microrobot-based desktop station for micro assembly and handling of micro-objects, IEEE Conf. on Emerging Technologies and Factory Automation (EFTA'96) (IEEE, Piscataway 1996) pp. 586–592

18.6 B.J. Nelson, Y. Zhou, B. Vikramaditya: Sensor-based microassembly of hybrid MEMS devices, IEEE Contr. Syst. Mag. **18**, 35–45 (1998)

18.7 K. Suzumori, T. Miyagawa, M. Kimura, Y. Hasegawa: Micro inspection robot for 1-in pipes, IEEE/ASME Trans. Mechatron. **4**, 286–292 (1999)

18.8 M. Takeda: Applications of MEMS to industrial inspection, Proc. 14th IEEE Int. Conf. on Micro Electro Mechanical Systems (IEEE, Piscataway 2001) pp. 182–191

18.9 T. Frank: Two-Axis electrodynamic micropositioning devices, J. Micromech. Microeng. **8**, 114–118 (1989)

18.10 N. Kawahara, N. Kawahara, T. Suto, T. Hirano, Y. Ishikawa, T. Kitahara, N. Ooyama, T. Ataka: Microfactories: New applications of micromachine technology to the manufacture of small products, Res. J. Microsyst. Technol. **3**, 37–41 (1997)

18.11 Y. Sun, B.J. Nelson: Microrobotic cell injection, Proc. of the 2001 IEEE International Conf. on Robotics and Automation (ICRA2001) (IEEE, Piscataway 2001) pp. 620–625

18.12 P. Dario, M.C. Carrozza, L. Lencioni, B. Magnani, S. Dapos Attanasio: A micro robotic system for colonoscopy, Proc. 1997 Int. Conf. on Robotics and Automation (IEEE, Piscataway 1997) pp. 1567–1572

18.13 F. Tendick, S.S. Sastry, R.S. Fearing, M. Cohn: Application of micromechatronics in minimally invasive surgery, IEEE/ASME Trans. Mechatron. **3**, 34–42 (1998)

18.14 G. Iddan, G. Meron, A. Glukhovsky, P. Swain: Wireless capsule endoscopy, Nature **405**, 417 (2000)

18.15 K.B. Yesin, K. Vollmers, B.J. Nelson: Analysis and design of wireless magnetically guided microrobots in body fluids, Proc. 2004 IEEE Int. Conf. on Robotics and Automation (IEEE, Piscataway 2004) pp. 1333–1338

18.16 M.C. Roco, R.S. Williams, P. Alivisatos: *Nanotechnology Research Directions: Interagency Working Group on Nanoscience, Engineering and Technology (IWGN) (Workshop Report)* (Kluwer, Dordrecht 2000)

18.17 M.L. Downey, D.T. Moore, G.R. Bachula, D.M. Etter, E.F. Carey, L.A. Perine: National Nanotechnology Initiative: Leading to the Next Industrial Revolution, A Report by the Interagency Working Group on Nanoscience, Engineering and Technology (Committee on Technology, National Science and Technology Council, Washington 2000)

18.18 K. Drexler: *Nanosystems: Molecular Machinery, Manufacturing and Computation* (Wiley, New York 1992)

18.19 G. Binnig, H. Rohrer, C. Gerber, E. Weibel: Surface studies by scanning tunneling microscopy, Phys. Rev. Lett. **49**, 57–61 (1982)

18.20 W.F. Degrado: Design of peptides and proteins, Adv. Protein Chem. **39**, 51–124 (1998)

18.21 G.M. Whitesides, B. Grzybowski: Self-assembly at all scales, Science **295**, 2418–2421 (2002)

18.22 R. Fearing: Survey of sticking effects for micro-parts, Proc. 1995 IEEE/RSJ Int. Conf. Int. Robots and Systems (IEEE, Piscataway 1995) pp. 212–217

18.23 E.L. Wolf: *Nanophysics and Nanotechnology* (WILEY-VCH, Weinheim 2004)

18.24 C.-J. Kim, A.P. Pisano, R.S. Muller: Silicon-processed overhanging microgripper, IEEE/ASME J. MEMS **1**, 31–36 (1992)

18.25 C. Liu, T. Tsao, Y.-C. Tai, C.-M. Ho: Surface micromachined magnetic actuators, Proc. 7th IEEE Int. Conf. Micro Electro Mechanical Systems (IEEE, Piscataway 1994) pp. 57–62

18.26 J. Judy, D.L. Polla, W.P. Robbins: A linear piezoelectric stepper motor with submicron displacement and centimeter travel, IEEE Trans. Ultrason. Ferroelectr. Freq. Contr. **37**, 428–437 (1990)

18.27 K. Nakamura, H. Ogura, S. Maeda, U. Sangawa, S. Aoki, T. Sato: Evaluation of the micro wobbler motor fabricated by concentric build-up process, Proc. 8th IEEE Int. Conf. Micro Electro Mechanical Systems (IEEE, Piscataway 1995) pp. 374–379

18.28 A. Teshigahara, M. Watanabe, N. Kawahara, I. Ohtsuka, T. Hattori: Performance of a 7-mm microfabricated car, IEEE/ASME J. MEMS **4**, 76–80 (1995)

18.29 K.R. Udayakumar, S.F. Bart, A.M. Flynn, J. Chen, L.S. Tavrow, L.E. Cross, R.A. Brooks, D.J. Ehrlich: Ferroelectric thin film ultrasonic micromotors, Proc. 4th IEEE Int. Conf. Micro Electro Mechanical Systems (IEEE, Piscataway 1991) pp. 109–113

18.30 T. Ebefors, G. Stemme: Microrobotics. In: *The MEMS Handbook*, ed. by M. Gad-el-Hak (CRC, Boca Raton 2002)

18.31 P. Dario, R. Valleggi, M.C. Carrozza, M.C. Montesi, M. Cocco: Review – Microactuators for microrobots:

A critical survey, J. Micromech. Microeng. **2**, 141–157 (1992)
18.32 I. Shimoyama: Scaling in microrobots, Proc. IEEE/RSJ Intelligent Robots and Systems (IEEE, Piscataway 1995) pp. 208–211
18.33 R.S. Fearing: Powering 3-dimensional microrobots: power density limitations, tutorial on "Micro Mechatronics and Micro Robotics", Proc. 1998 IEEE Int. Conf. on Robotics and Automation (IEEE, Piscataway 1998)
18.34 R.G. Gilbertson, J.D. Busch: A survey of micro-actuator technologies for future spacecraft missions, J. Br. Interplanet. Soc. **49**, 129–138 (1996)
18.35 M. Mehregany, P. Nagarkar, S.D. Senturia, J.H. Lang: Operation of microfabricated harmonic and ordinary side-drive motors, Proc. 3rd IEEE Int. Conf. Micro Electro Mechanical Systems (IEEE, Piscataway 1990) pp. 1–8
18.36 Y.C. Tai, L.S. Fan, R.S. Mulle: IC-processed micro-motors: design, technology, and testing, Proc. 2nd IEEE Int. Conf. Micro Electro Mechanical Systems (IEEE, Piscataway 1989) pp. 1–6
18.37 T. Ohnstein, T. Fukiura, J. Ridley, U. Bonne: Micromachined silicon microvalve, Proc. 3rd IEEE Int. Conf. Micro Electro Mechanical Systems (IEEE, Piscataway 1990) pp. 95–99
18.38 L.Y. Chen, S.L. Zhang, J.J. Yao, D.C. Thomas, N.C. MacDonald: Selective chemical vapor deposition of tungsten for microdynamic structures, Proc. 2nd IEEE Int. Conf. Micro Electro Mechanical Systems (IEEE, Piscataway 1989) pp. 82–87
18.39 K. Yanagisawa, H. Kuwano, A. Tago: An electromagnetically driven microvalve, Proc. 7th Int. Conf. on Solid-State Sensors and Actuators (IEEE, Piscataway 1993) pp. 102–105
18.40 M. Esashi, S. Shoji, A. Nakano: Normally close microvalve and micropump fabricated on a silicon wafer, Proc. 2nd IEEE Int. Conf. Micro Electro Mechanical Systems (IEEE, Piscataway 1989) pp. 29–34
18.41 R. Petrucci, K. Simmons: An introduction to piezoelectric crystals. In: *Sensors Magazine* (Helmers, Peterborough 1994) pp. 26–
18.42 J. Goldstein, D. Newbury, D. Joy, C. Lyman, P. Echlin, E. Lifshin, L. Sawyer, J. Michael: *Scanning Electron Microscopy and X-ray Microanalysis* (Kluwer Academic/Plenum, New York 2003)
18.43 G. Binnig, H. Rohrer: In touch with atoms, Rev. Mod. Phys. **71**, S324–S330 (1999)
18.44 G. Binnig, C.F. Quate, C. Gerber: Atomic force microscope, Phys. Rev. Lett. **56**, 93–96 (1986)
18.45 M.J. Doktycz, C.J. Sullivan, P.R. Hoyt, D.A. Pelletier, S. Wu, D.P. Allison: AFM imaging of bacteria in liquid media immobilized on gelatin coated mica surfaces, Ultramicroscopy **97**, 209–216 (2003)
18.46 S.A. Campbell: *The Science and Engineering of Microelectronic Fabrication* (Oxford Univ. Press, New York 2001)
18.47 C.J. Jaeger: *Introduction to Microelectronic Fabrication* (Prentice Hall, Upper Saddle River 2002)
18.48 J.D. Plummer, M.D. Deal, P.B. Griffin: *Silicon VLSI Technology* (Prentice Hall, Upper Saddle River 2000)
18.49 M. Gad-el-Hak(Ed.): *The MEMS Handbook* (CRC, Boca Raton 2002)
18.50 T.-R. Hsu: *MEMS and Microsystems Design and Manufacture* (McGraw-Hill, New York 2002)
18.51 G.T.A. Kovacs: *Micromachined Transducers Sourcebook* (McGraw-Hill, New York 1998)
18.52 G.T.A. Kovacs, N.I. Maluf, K.A. Petersen: Bulk micromachining of silicon, Proc. IEEE Int. Conf. Robot. Autom. **86**, 1536–1551 (1998)
18.53 P. Rai-Choudhury (Ed.): *Handbook of Microlithography, Micromachining and Microfabrication* (SPIE, Bellingham 1997)
18.54 S.Y. Chou: Nano-imprint lithography and lithographically induced self-assembly, MRS Bull. **26**, 512–517 (2001)
18.55 M.A. Herman: *Molecular Beam Epitaxy: Fundamentals and Current Status* (Springer, New York 1996)
18.56 J.S. Frood, G.J. Davis, W.T. Tsang: *Chemical Beam Epitaxy and Related Techniques* (Wiley, New York 1997)
18.57 S. Mahajan, K.S.S. Harsha: *Principles of Growth and Processing of Semiconductors* (McGraw-Hill, New York 1999)
18.58 C.A. Mirkin: Dip-pen nanolithography: automated fabrication of custom multicomponent, sub-100 nanometer surface architectures, MRS Bull. **26**, 535–538 (2001)
18.59 C.A. Harper: *Electronic Packaging and Interconnection Handbook* (McGraw-Hill, New York 2000)
18.60 K.F. Bohringer, R.S. Fearing, K.Y. Goldberg: Microassembly. In: *Handbook of Industrial Robotics*, ed. by S. Nof (Wiley, New York 1999) pp. 1045–1066
18.61 G. Yang, J.A. Gaines, B.J. Nelson: A supervisory wafer-level 3D microassembly system for hybrid MEMS fabrication, J. Intell. Robot. Syst. **37**, 43–68 (2003)
18.62 P. Dario, M. Carrozza, N. Croce, M. Montesi, M. Cocco: Non-traditional technologies for microfabrication, J. Micromech. Microeng. **5**, 64–71 (1995)
18.63 W. Benecke: Silicon microactuators: activation mechanisms and scaling problems, Proc. IEEE Int. Conf. Solid-State Sensors and Actuators (IEEE, Piscataway 1991) pp. 46–50
18.64 A. Menciassi, A. Eisinberg, M. Mazzoni, P. Dario: A sensorized electro discharge machined superelastic alloy microgripper for micromanipulation: simulation and characterization, Proc. 2002 IEEE/RSJ Int. Conf. Intelligent Robots and Systems (IEEE, Piscataway 2002) pp. 1591–1595
18.65 T.R. Hsu: Packaging design of microsystems and meso-scale devices, IEEE Trans. Adv. Packag. **23**, 596–601 (2000)

18.66 L. Lin: MEMS post-packaging by localized heating and bonding, IEEE Trans. Adv. Packag. **23**, 608–616 (2000)

18.67 A. Tixier, Y. Mita, S. Oshima, J.P. Gouy, H. Fujita: 3-D microsystem packaging for interconnecting electrical, optical and mechanical microdevices to the external world, Proc. 13th IEEE Int. Conf. Micro Electro Mechanical Systems (IEEE, Piscataway 2000) pp. 698–703

18.68 M.J. Madou: *Fundamentals of Microfabrication* (CRC, Boca Raton 2002)

18.69 I. Shimoyama, O. Kano, H. Miura: 3D microstructures folded by Lorentz force, Proc. 11th IEEE Int. Conf. Micro Electro Mechanical Systems (IEEE, Piscataway 1998) pp. 24–28

18.70 K.F. Bohringer, B.R. Donald, L. Kavraki, F.L. Lamiraux: Part orientation with one or two stable equilibria using programmable vector fields, IEEE Trans. Robot. Autom. **16**, 157–170 (2000)

18.71 V. Kaajakari, A. Lal: An electrostatic batch assembly of surface MEMS using ultrasonic triboelectricity, Proc. 14th IEEE Int. Conf. Micro Electro Mechanical Systems (IEEE, Piscataway 2001) pp. 10–13

18.72 G. Yang, B.J. Nelson: Micromanipulation contact transition control by selective focusing and microforce control, Proc. 2003 IEEE Int. Conf. on Robotics and Automation (IEEE, Piscataway 2003) pp. 3200–3206

18.73 G. Morel, E. Malis, S. Boudet: Impedance based combination of visual and force control, Proc. 1998 IEEE Int. Conf. on Robotics and Automation (IEEE, Piscataway 1998) pp. 1743–1748

18.74 F. Arai, D. Andou, T. Fukuda: Adhesion forces reduction for micro manipulation based on micro physics, Proc. 9th IEEE Int. Conf. Micro Electro Mechanical Systems (IEEE, Piscataway 1996) pp. 354–359

18.75 Y. Zhou, B.J. Nelson: The effect of material properties and gripping force on micrograsping, Proc. 2000 IEEE Int. Conf. Robotics and Automation (IEEE, Piscataway 2000) pp. 1115–1120

18.76 K. Kurata: Mass production techniques for optical modules, Proc. 48th IEEE Electronic Components and Technology Conf. (IEEE, Piscataway 1998) pp. 572–580

18.77 V.T. Portman, B.-Z. Sandler, E. Zahavi: Rigid 6 × 6 parallel platform for precision 3-D micromanipulation: theory and design application, IEEE Trans. Robot. Autom. **16**, 629–643 (2000)

18.78 R.M. Haralick, L.G. Shapiro: *Computer and Robot Vision* (Addison-Wesley, Reading 1993)

18.79 A. Khotanzad, H. Banerjee, M.D. Srinath: A vision system for inspection of ball bonds and 2-D profile of bonding wires in integrated circuits, IEEE Trans. Semicond. Manuf. **7**, 413–422 (1994)

18.80 J.T. Feddema, R.W. Simon: CAD-driven microassembly and visual servoing, Proc. 1998 IEEE Int. Conf. Robotics and Automation (IEEE, Piscataway 1998) pp. 1212 -1219

18.81 E. Trucco, A. Verri: *Introductory Techniques for 3-D Computer Vision* (Prentice Hall, Upper Saddle River 1998)

18.82 S. Hutchinson, G.D. Hager, P.I. Corke: A tutorial on visual servo control, IEEE Trans. Robot. Autom. **12**, 651–670 (1996)

18.83 B. Siciliano, L. Villani: *Robot Force Control* (Kluwer, Dordrecht 2000)

18.84 T. Yoshikawa: Force control of robot manipulators, Proc. 2000 IEEE Int. Conf. Robotics and Automation (IEEE, Piscataway 2000) pp. 220–226

18.85 J.A. Thompson, R.S. Fearing: Automating microassembly with ortho-tweezers and force sensing, Proc. 2001 IEEE/RSJ Int. Conf. Int. Robots and Systems (IEEE, Piscataway 2001) pp. 1327–1334

18.86 B.J. Nelson, P.K. Khosla: Force and vision resolvability for assimilating disparate sensory feedback, IEEE Trans. Robot. Autom. **12**, 714–731 (1996)

18.87 Y. Haddab, N. Chaillet, A. Bourjault: A microgripper using smart piezoelectric actuators, Proc. 2000 IEEE/RSJ Int. Conf. Intelligent Robots and Systems (IEEE, Piscataway 2000) pp. 659–664

18.88 D. Popa, B.H. Kang, J. Sin, J. Zou: Reconfigurable micro-assembly system for photonics applications, Proc. 2002 IEEE Int. Conf. Robotics and Automation (IEEE, Piscataway 2002) pp. 1495–1500

18.89 A.P. Lee, D.R. Ciarlo, P.A. Krulevitch, S. Lehew, J. Trevin, M.A. Northrup: A practical microgripper by fine alignment, eutectic bonding and SMA actuation, Transducers'95 (IEEE, Piscataway 1995) pp. 368–371

18.90 H. Seki: Modeling and impedance control of a piezoelectric bimorph microgripper, Proc. 1992 IEEE/RSJ Int. Conf. Intelligent Robots and Systems (IEEE, Piscataway 1992) pp. 958–965

18.91 W. Nogimori, K. Irisa, M. Ando, Y. Naruse: A laser-powered micro-gripper, Proc. 10th IEEE Int. Conf. Micro Electro Mechanical Systems (IEEE, Piscataway 1997) pp. 267–271

18.92 S. Fatikow, U. Rembold: *Microsystem Technology and Microrobotics* (Springer, Berlin, Heidelberg 1997)

18.93 T. Hayashi: Micro mechanism, J. Robot. Mechatr. **3**, 2–7 (1991)

18.94 S. Johansson: Micromanipulation for micro- and nanomanufacturing, INRIA/IEEE Symp. on Emerging Technologies and Factory Automation (ETFA'95), Paris (1995) pp. 3–8

18.95 K.-T. Park, M. Esashi: A multilink active catheter with polyimide-based integrated CMOS interface circuits, J. MEMS **8**, 349–357 (1999)

18.96 Y. Haga, Y. Tanahashi, M. Esashi: Small diameter active catheter using shape memory alloy, Proc. IEEE 11th Int. Workshop on Micro Electro Mechanical Systems, Heidelberg (1998) pp. 419–424

18.97 E.W.H. Jager, O. Inganas, I. Lundstrom: Microrobots for micrometer-size objects in aqueous media: Potential tools for single cell manipulation, Science **288**, 2335–2338 (2000)

18.98 E.W.H. Jager, E. Smela, O. Inganas: Microfabricating conjugated polymer actuators, Science **290**, 1540–1545 (2000)

18.99 J.W. Suh, S.F. Glander, R.B. Darling, C.W. Storment, G.T.A. Kovacs: Organic thermal and electrostatic ciliary microactuator array for object manipulation, Sens. Actuat. A **58**, 51–60 (1997)

18.100 E. Smela, M. Kallenbach, J. Holdenried: Electrochemically driven polypyrrole bilayers for moving and positioning bulk micromachined silicon plates, J. MEMS **8**, 373–383 (1999)

18.101 S. Konishi, H. Fujita: A conveyance system using air flow based on the concept of distributed micro motion systems, IEEE J. MEMS **3**, 54–58 (1994)

18.102 M. Ataka, A. Omodaka, N. Takeshima, H. Fujita: Fabrication and operation of polyimide bimorph actuators for a ciliary motion system, J. MEMS **2**, 146–150 (1993)

18.103 G.-X. Zhou: Swallowable or implantable body temperature telemeter-body temperature radio pill, Proc. IEEE 15th Annual Northeast Bioengineering Conf. (1989) pp. 165–166

18.104 A. Uchiyama: Endoradiosonde Needs Micro Machine Technology, Proc. IEEE 6th Int. Symp. on Micro Machine and Human Science (MHS '95) (IEEE, Nagoya 1995) pp. 31–37

18.105 Y. Carts-Powell: Tiny Camera in a Pill Extends Limits of Endoscopy, SPIE: OE-Reports Aug. (2000) (available on Internet at: http://www.spie.org)

18.106 R. Yeh, E.J.J. Kruglick, K.S.J. Pister: Surface-micromachined components for articulated microrobots, J. MEMS **5**, 10–17 (1996)

18.107 P.E. Kladitis, V.M. Bright, K.F. Harsh, Y.C. Lee: Prototype Microrobots for micro positioning in a manufacturing process and micro unmanned vehicles, Proc. IEEE 12th Int. Conf. on Micro Electro Mechanical Systems (MEMS'99), Oralndo (1999) pp. 570–575

18.108 D. Ruffieux, N.F. d. Rooij: A 3-DoF bimorph actuator array capable of locomotion, 13th European Conf. on Solid-State Transducers (Eurosensors XIII), Hague (1999) pp. 725–728

18.109 J.-M. Breguet, P. Renaud: A 4 degrees-of-freedoms microrobot with nanometer resolution, Robotics **14**, 199–203 (1996)

18.110 A. Flynn, L.S. Tavrow, S.F. Bart, R.A. Brooks, D.J. Ehrlich, K.R. Udayakumar, L.E. Cross: Piezoelectric micromotors for microrobots, IEEE J. MEMS **1**, 44–51 (1992)

18.111 A. Teshigahara, M. Watanabe, N. Kawahara, Y. Ohtsuka, T. Hattori: Performance of a 7 mm microfabricated car, IEEE/ASME J. MEMS **4**, 76–80 (1995)

18.112 T. Ebefors, J. Mattson, E. Kalvesten, G. Stemme: A walking silicon micro-robot, 10th Int. Conf. on Solid-State Sensors and Actuators (Transducers'99), Sendai (1999) pp. 1202–1205

18.113 N. Miki, I. Shimoyama: Flight performance of micro-wings rotating in an alternating magnetic field, Proc. IEEE 12th Int. Conf. on Micro Electro Mechanical Systems (MEMS'99), Oralndo (1999) pp. 153–158

18.114 Mainz: Micro-motors: The World's Tiniest Helicopter, in http://www.imm-mainz.de/english/developm/products/hubi.html Orlando (1999)

18.115 K.I. Arai, W. Sugawara, T. Honda: *Magnetic small flying machines*, Tech. Digest Transducers'95 and Eurosensors IX, Stockholm (1995) pp. 316–319

18.116 T. Fukuda, A. Kawamoto, F. Arai, H. Matsuura: Mechanism and swimming experiment of micro mobile robot in water, Proc. IEEE 7th Int. Workshop on Micro Electro Mechanical Systems (MEMS'94), Oiso (1994) pp. 273–278

18.117 I. Shimoyama: Hybrid system of mechanical parts and living organisms for microrobots, Proc. IEEE 6th Int. Symp. on Micro Machine and Human Science (MHS '95) (IEEE, Nagoya 1995) p. 55

18.118 A. Ashkin: Acceleration and trapping of particles by radiation pressure, Phys. Rev. Lett. **24**, 156–159 (1970)

18.119 T.N. Bruican, M.J. Smyth, H.A. Crissman, G.C. Salzman, C.C. Stewart, J.C. Martin: Automated single-cell manipulation and sorting by light trapping, Appl. Opt. **26**, 5311–5316 (1987)

18.120 J. Conia, B.S. Edwards, S. Voelkel: The microrobotic laboratory: Optical trapping and scissing for the biologist, J. Clin. Lab. Anal. **11**, 28–38 (1997)

18.121 W.H. Wright, G.J. Sonek, Y. Tadir, M.W. Berns: Laser trapping in cell biology, IEEE J. Quant. Electron. **26**, 2148–2157 (1990)

18.122 F. Arai, K. Morishima, T. Kasugai, T. Fukuda: Biomicromanipulation (new direction for operation improvement), Proc. of 1997 IEEE/RSJ Int. Conf. on Intelligent Robotics and Systems (IEEE, Piscataway 1997) pp. 1300–1305

18.123 M. Nishioka, S. Katsura, K. Hirano, A. Mizuno: Evaluation of cell characteristics by step-wise orientational rotation using optoelectrostatic micromanipulation, IEEE Trans. Ind. Appl. **33**, 1381–1388 (1997)

18.124 M. Washizu, Y. Kurahashi, H. Iochi, O. Kurosawa, S. Aizawa, S. Kudo, Y. Magariyama, H. Hotani: Dielectrophoretic measurement of bacterial motor characteristics, IEEE Trans. Ind. Appl. **29**, 286–294 (1993)

18.125 Y. Kimura, R. Yanagimachi: Intracytoplasmic sperm injection in the mouse, Biol. Reprod. **52**, 709–720 (1995)

18.126 M. Mischel, A. Voss, H.A. Pohl: Cellular spin resonance in rotating electric fields, J. Biol. Phys. **10**, 223–226 (1982)

18.127 W.M. Arnold, U. Zimmermann: Electro-Rotation: Development of a technique for dielectric measurements on individual cells and particles, J. Electrost. **21**, 151–191 (1988)

18.128 Y. Sun, B.J. Nelson: Autonomous injection of biological cells using visual servoing, Int. Symp. on Experimental Robotics (ISER 2000), Lect. Notes Contr. Inform. Sci. (2000) pp. 175–184

18.129 Y. Sun, B.J. Nelson, D.P. Potasek, E. Enikov: A bulk microfabricated multi-axis capacitive cellular force sensor using transverse comb drives, J. Micromech. Microeng. **12**, 832–840 (2002)

18.130 Y. Sun, K. Wan, K.P. Roberts, J.C. Bischof, B.J. Nelson: Mechanical property characterization of mouse zona pellucida, IEEE Trans. Nanobiosci. **2**, 279–286 (2003)

18.131 A. Ashkin, J.M. Dziedzic: Optical trapping and manipulation of viruses and bacteria, Science **235**, 1517–1520 (1987)

18.132 F.H.C. Crick, A.F.W. Hughes: The physical properties of cytoplasm: A study by means of the magnetic particle method, Part I. Experimental Exp. Cell Res. **1**, 37–80 (1950)

18.133 M.F. Yu, M.J. Dyer, G.D. Skidmore, H.W. Rohrs, X.K. Lu, K.D. Ausman, J.R.V. Ehr, R.S. Ruoff: Three-dimensional manipulation of carbon nanotubes under a scanning electron microscope, Nanotechnology **10**, 244–252 (1999)

18.134 L.X. Dong, F. Arai, T. Fukuda: 3D nanorobotic manipulation of nano-order objects inside SEM, Proc. of 2000 Int. Symp. on Micromechatronics and Human Science (MHS2000) (IEEE, Piscataway 2000) pp. 151–156

18.135 D.M. Eigler, E.K. Schweizer: Positioning single atoms with a scanning tunneling microscope, Nature **344**, 524–526 (1990)

18.136 P. Avouris: Manipulation of matter at the atomic and molecular levels, Acc. Chem. Res. **28**, 95–102 (1995)

18.137 M.F. Crommie, C.P. Lutz, D.M. Eigler: Confinement of electrons to quantum corrals on a metal surface, Science **262**, 218–220 (1993)

18.138 L.J. Whitman, J.A. Stroscio, R.A. Dragoset, R.J. Cellota: Manipulation of adsorbed atoms and creation of new structures on room-temperature surfaces with a scanning tunneling microscope, Science **251**, 1206–1210 (1991)

18.139 I.-W. Lyo, P. Avouris: Field-induced nanometer-scale to atomic-scale manipulation of silicon surfaces with the STM, Science **253**, 173–176 (1991)

18.140 G. Dujardin, R.E. Walkup, P. Avouris: Dissociation of individual molecules with electrons from the tip of a scanning tunneling microscope, Science **255**, 1232–1235 (1992)

18.141 T.-C. Shen, C. Wang, G.C. Abeln, J.R. Tucker, J.W. Lyding, P. Avouris, R.E. Walkup: Atomic-scale desorption through electronic and vibrational-excitation mechanisms, Science **268**, 1590–1592 (1995)

18.142 M.T. Cuberes, R.R. Schittler, J.K. Gimzewsk: Room-temperature repositioning of individual C60 molecules at Cu steps: operation of a molecular counting device, Appl. Phys. Lett. **69**, 3016–3018 (1996)

18.143 H.J. Lee, W. Ho: Single-bond formation and characterization with a scanning tunneling microscope, Science **286**, 1719–1722 (1999)

18.144 T. Yamamoto, O. Kurosawa, H. Kabata, N. Shimamoto, M. Washizu: Molecular surgery of DNA based on electrostatic micromanipulation, IEEE Trans. IA **36**, 1010–1017 (2000)

18.145 C. Haber, D. Wirtz: Magnetic tweezers for DNA micromanipulation,, Rev. Sci. Instrum. **71**, 4561–4570 (2000)

18.146 D.M. Schaefer, R. Reifenberger, A. Patil, R.P. Andres: Fabrication of two-dimensional arrays of nanometer-size clusters with the atomic force microscope, Appl. Phys. Lett. **66**, 1012–1014 (1995)

18.147 T. Junno, K. Deppert, L. Montelius, L. Samuelson: Controlled manipulation of nanoparticles with an atomic force microscope, Appl. Phys. Lett. **66**, 3627–3629 (1995)

18.148 P.E. Sheehan, C.M. Lieber: Nanomachining, manipulation and fabrication by force microscopy, Nanotechnology **7**, 236–240 (1996)

18.149 C. Baur, B.C. Gazen, B. Koel, T.R. Ramachandran, A.A.G. Requicha, L. Zini: Robotic nanomanipulation with a scanning probe microscope in a networked computing environment, J. Vac. Sci. Tech. B **15**, 1577–1580 (1997)

18.150 A.A.G. Requicha: Nanorobots, NEMS, and nanoassembly, Proc. IEEE **91**, 1922–1933 (2003)

18.151 R. Resch, C. Baur, A. Bugacov, B.E. Koel, A. Madhukar, A.A.G. Requicha, P. Will: Building and manipulating 3-D and linked 2-D structures of nanoparticles using scanning force microscopy, Langmuir **14**, 6613–6616 (1998)

18.152 J. Hu, Z.-H. Zhang, Z.-Q. Ouyang, S.-F. Chen, M.-Q. Li, F.-J. Yang: Stretch and align virus in nanometer scale on an atomically flat surface, J. Vac. Sci. Tech. B **16**, 2841–2843 (1998)

18.153 M. Sitti, S. Horiguchi, H. Hashimoto: Controlled pushing of nanoparticles: modeling and experiments, IEEE/ASME Trans. Mechatron. **5**, 199–211 (2000)

18.154 M. Guthold, M.R. Falvo, W.G. Matthews, S. Paulson, S. Washburn, D.A. Erie, R. Superfine, J.F.P. Brooks, I.R.M. Taylor: Controlled manipulation of molecular samples with the nanoManipulator, IEEE/ASME Trans. Mechatron. **5**, 189–198 (2000)

18.155 G.Y. Li, N. Xi, M.M. Yu, W.K. Fung: Development of augmented reality system for AFM-based nanomanipulation, IEEE/ASME Trans. Mechatron. **9**, 358–365 (2004)

18.156 F. Arai, D. Andou, T. Fukuda: Micro manipulation based on micro physics–strategy based on attractive force reduction and stress measurement, Proc. of IEEE/RSJ Int. Conf. on Intelligent Robotics and Systems (IEEE, Piscataway 1995) pp. 236–241

18.157 H.W.P. Koops, J. Kretz, M. Rudolph, M. Weber, G. Dahm, K.L. Lee: Characterization and application of materials grown by electron-beam-induced deposition, Jpn. J. Appl. Phys. **33**, 7099–7107 (1994), Part 1

18.158 S. Iijima: Helical microtubules of graphitic carbon, Nature **354**, 56–58 (1991)

18.159 S.J. Tans, A.R.M. Verchueren, C. Dekker: Room-temperature transistor based on a single carbon nanotube, Nature **393**, 49–52 (1998)

18.160 R.H. Baughman, A.A. Zakhidov, W.A. de Heer: Carbon nanotubes-the route toward applications, Science **297**, 787–792 (2002)

18.161 M.J. Treacy, T.W. Ebbesen, J.M. Gibson: Exceptionally high Young's modulus observed for individual carbon nanotubes, Nature **381**, 678–680 (1996)

18.162 P. Poncharal, Z.L. Wang, D. Ugarte, W.A. de Heer: Electrostatic deflections and electromechanical resonances of carbon nanotubes, Science **283**, 1513–1516 (1999)

18.163 M.F. Yu, O. Lourie, M.J. Dyer, K. Moloni, T.F. Kelley, R.S. Ruoff: Strength and breaking mechanism of multiwalled carbon nanotubes under tensile load, Science **287**, 637–640 (2000)

18.164 T.W. Ebbesen, H.J. Lezec, H. Hiura, J.W. Bennett, H.F. Ghaemi, T. Thio: Electrical conductivity of individual carbon nanotubes, Nature **382**, 54–56 (1996)

18.165 P. Kim, L. Shi, A. Majumdar, P.L. McEuen: Thermal transport measurements of individual multiwalled nanotubes, Phys. Rev. Lett. **87**, 215502 (2001)

18.166 W.J. Liang, M. Bockrath, D. Bozovic, J.H. Hafner, M. Tinkham, H. Park: Fabry-Perot interference in a nanotube electron waveguide, Nature **411**, 665–669 (2001)

18.167 X.B. Zhang, D. Bernaerts, G.V. Tendeloo, S. Amelincks, J.V. Landuyt, V. Ivanov, J.B. Nagy, P. Lambin, A.A. Lucas: The texture of catalytically grown coil-shaped carbon nanotubules, Europhys. Lett. **27**, 141–146 (1994)

18.168 X.Y. Kong, Z.L. Wang: Spontaneous polarization-induced nanohelixes, nanosprings, and nanorings of piezoelectric nanobelts, Nano. Lett. **3**, 1625–1631 (2003)

18.169 S.V. Golod, V.Y. Prinz, V.I. Mashanov, A.K. Gutakovsky: Fabrication of conducting GeSi/Si micro- and nanotubes and helical microcoils, Semicond. Sci. Technol. **16**, 181–185 (2001)

18.170 L. Zhang, E. Deckhardt, A. Weber, C. Schönenberger, D. Grützmacher: Controllable fabrication of SiGe/Si and SiGe/Si/Cr helical nanobelts, Nanotechnology **16**, 655–663 (2005)

18.171 L. Zhang, E. Ruh, D. Grützmacher, L.X. Dong, D.J. Bell, B.J. Nelson, C. Schönenberger: Anomalous coiling of SiGe/Si and SiGe/Si/Cr helical nanobelts, Nano Lett. **6**, 1311–1317 (2006)

18.172 D.J. Bell, L.X. Dong, B.J. Nelson, M. Golling, L. Zhang, D. Grützmacher: Fabrication and characterization of three-dimensional InGaAs/GaAs nanosprings, Nano Lett. **6**, 725–729 (2006)

18.173 D.J. Bell, Y. Sun, L. Zhang, L.X. Dong, B.J. Nelson, D. Grutzmacher: Three-dimensional nanosprings for electromechanical sensors, Sens. Actuat. A-Physical **130**, 54–61 (2006)

18.174 R. Martel, T. Schmidt, H.R. Shea, T. Herte, P. Avouris: Single- and multi-wall carbon nanotube field-effect transistors, Appl. Phys. Lett. **73**, 2447–2449 (1998)

18.175 N.R. Franklin, Y.M. Li, R.J. Chen, A. Javey, H.J. Dai: Patterned growth of single-walled carbon nanotubes on full 4-inch wafers, Appl. Phys. Lett. **79**, 4571–4573 (2001)

18.176 T. Rueckes, K. Kim, E. Joselevich, G.Y. Tseng, C.-L. Cheung, C.M. Lieber: Carbon nanotube-based non-volatile random access memory for molecular computing science, Science **289**, 94–97 (2000)

18.177 A. Subramanian, B. Vikramaditya, L.X. Dong, D.J. Bell, B.J. Nelson: Micro and Nanorobotic Assembly Using Dielectrophoresis. In: *Robotics: Science and Systems I*, ed. by S. Thrun, G.S. Sukhatme, S. Schaal, O. Brock (MIT Press, Cambridge 2005) pp. 327–334

18.178 C.K.M. Fung, V.T.S. Wong, R.H.M. Chan, W.J. Li: Dielectrophoretic batch fabrication of bundled carbon nanotube thermal sensors, IEEE Trans. Nanotech. **3**, 395–403 (2004)

18.179 T. Fukuda, F. Arai, L.X. Dong: Assembly of nanodevices with carbon nanotubes through nanorobotic manipulations, Proc. IEEE **91**, 1803–1818 (2003)

18.180 E.W. Wong, P.E. Sheehan, C.M. Lieber: Nanobeam mechanics: elasticity, strength, and toughness of nanorods and nanotubes, Science **277**, 1971–1975 (1997)

18.181 M.R. Falvo, G.J. Clary, R.M. Taylor, V. Chi, F.P. Brooks, S. Washburn, R. Superfine: Bending and buckling of carbon nanotubes under large strain, Nature **389**, 582–584 (1997)

18.182 H.W.C. Postma, A. Sellmeijer, C. Dekker: Manipulation and imaging of individual single-walled carbon nanotubes with an atomic force microscope, Adv. Mater. **12**, 1299–1302 (2000)

18.183 T. Hertel, R. Martel, P. Avouris: Manipulation of individual carbon nanotubes and their interaction with surfaces, J. Phys. Chem. B **102**, 910–915 (1998)

18.184 P. Avouris, T. Hertel, R. Martel, T. Schmidt, H.R. Shea, R.E. Walkup: Carbon nanotubes: nanomechanics, manipulation, and electronic devices, Appl. Surf. Sci. **141**, 201–209 (1999)

18.185 M. Ahlskog, R. Tarkiainen, L. Roschier, P. Hakonen: Single-electron transistor made of two crossing multiwalled carbon nanotubes and its noise properties, Appl. Phys. Lett. **77**, 4037–4039 (2000)

18.186 M.R. Falvo, R.M.I. Taylor, A. Helser, V. Chi, F.P.J. Brooks, S. Washburn, R. Superfine: Nanometre-scale rolling and sliding of carbon nanotubes, Nature **397**, 236–238 (1999)

18.187 B. Bhushan, V.N. Koinkar: Nanoindentation Hardness Measurements Using Atomic-Force Microscopy, Appl. Phys. Lett. **64**, 1653–1655 (1994)

18.188 P. Vettiger, G. Cross, M. Despont, U. Drechsler, U. Durig, B. Gotsmann, W. Haberle, M.A. Lantz, H.E. Rothuizen, R. Stutz, G.K. Binnig: The "millipede" – Nanotechnology entering data storage, IEEE Trans. Nanotechnol. **1**, 39–55 (2002)

18.189 L.X. Dong: Nanorobotic manipulations of carbon nanotubes. Ph.D. Thesis (Nagoya University, Nagoya 2003)

18.190 J.H. Hafner, C.-L. Cheung, T.H. Oosterkamp, C.M. Lieber: High-yield assembly of individual single-walled carbon nanotube tips for scanning probe microscopies, J. Phys. Chem. B **105**, 743–746 (2001)

18.191 L.X. Dong, F. Arai, T. Fukuda: Electron-beam-induced deposition with carbon nanotube emitters, Appl. Phys. Lett. **81**, 1919–1921 (2002)

18.192 L.X. Dong, F. Arai, T. Fukuda: 3D nanorobotic manipulations of multi-walled carbon nanotubes, Proc. of 2001 IEEE Int. Conf. on Robotics and Automation (ICRA2001) (IEEE, Piscataway 2001) pp. 632–637

18.193 L.X. Dong, F. Arai, T. Fukuda: Destructive constructions of nanostructures with carbon nanotubes through nanorobotic manipulation, IEEE/ASME Trans. Mechatron. **9**, 350–357 (2004)

18.194 J. Cumings, P.G. Collins, A. Zettl: Peeling and sharpening multiwall nanotubes, Nature **406**, 58 (2000)

18.195 J. Cumings, A. Zettl: Low-friction nanoscale linear bearing realized from multiwall carbon nanotubes, Science **289**, 602–604 (2000)

18.196 A. Kis, K. Jensen, S. Aloni, W. Mickelson, A. Zettl: Interlayer forces and ultralow sliding friction in multiwalled carbon nanotubes, Phys. Rev. Lett. **97**, 025501 (2006)

18.197 L.X. Dong, F. Arai, T. Fukuda: Nanoassembly of carbon nanotubes through mechanochemical nanorobotic manipulations, Jpn. J. Appl. Phys. **42**, 295–298 (2003), Part 1

18.198 L. Chico, V.H. Crespi, L.X. Benedict, S.G. Louie, M.L. Cohen: Pure carbon nanoscale devices: Nanotube heterojunctions, Phys. Rev. Lett. **76**, 971–974 (1996)

18.199 Z. Yao, H.W.C. Postma, L. Balents, C. Dekker: Carbon nanotube intramolecular junctions, Nature **402**, 273–276 (1999)

18.200 H.W.C. Postma, T. Teepen, Z. Yao, M. Grifoni, C. Dekker: Carbon nanotube single-electron transistors at room temperature, Science **293**, 76–79 (2001)

18.201 M.S. Fuhrer, J. Nygård, L. Shih, M. Forero, Y.-G. Yoon, M.S.C. Mazzoni, H.J. Choi, J. Ihm, S.G. Louie, A. Zettl, P.L. McEuen: Crossed nanotube junctions, Science **288**, 494–497 (2000)

18.202 T. Rueckes, K. Kim, E. Joselevich, G.Y. Tseng, C.-L. Cheung, C.M. Lieber: Carbon nanotube-based nonvolatile random access memory for molecular computing science, Science **289**, 94–97 (2000)

18.203 A.G. Rinzler, J.H. Hafner, P. Nikolaev, L. Lou, S.G. Kim, D. Tománek, P. Nordlander, D.T. Colbert, R.E. Smalley: Unraveling nanotubes: field emission from an atomic wire, Science **269**, 1550–1553 (1995)

18.204 S.C. Minne, G. Yaralioglu, S.R. Manalis, J.D. Adams, J. Zesch, A. Atalar, C.F. Quate: Automated parallel high-speed atomic force microscopy, Appl. Phys. Lett. **72**, 2340–2342 (1998)

18.205 G.D. Skidmore, E. Parker, M. Ellis, N. Sarkar, R. Merkle: Exponential assembly, Nanotechnology **11**, 316–321 (2001)

18.206 H.J. Dai, J.H. Hafner, A.G. Rinzler, D.T. Colbert, R.E. Smalley: Nanotubes as nanoprobes in scanning probe microscopy, Nature **384**, 147–150 (1996)

18.207 J.H. Hafner, C.L. Cheung, C.M. Lieber: Growth of nanotubes for probe microscopy tips, Nature **398**, 761–762 (1999)

18.208 L.X. Dong, B.J. Nelson, T. Fukuda, F. Arai: Towards Nanotube Linear Servomotors, IEEE Trans. Autom. Sci. Eng. **3**, 228–235 (2006)

18.209 Y.H. Gao, Y. Bando: Carbon nanothermometer containing gallium, Nature **415**, 599 (2002)

18.210 L.X. Dong, X.Y. Tao, L. Zhang, B.J. Nelson, X.B. Zhang: Nanorobotic spot welding: Controlled metal deposition with attogram precision from Copper-filled carbon nanotubes, Nano Lett. **7**, 58–63 (2007)

18.211 S.W. Lee, D.S. Lee, R.E. Morjan, S.H. Jhang, M. Sveningsson, O.A. Nerushev, Y.W. Park, E.E.B. Campbell: A three-terminal carbon nanorelay, Nano Lett. **4**, 2027–2030 (2004)

18.212 A.M. Fennimore, T.D. Yuzvinsky, W.-Q. Han, M.S. Fuhrer, J. Cumings, A. Zettl: Rotational actuators based on carbon nanotubes, Nature **424**, 408–410 (2003)

18.213 A. Subramanian, L.X. Dong, J. Tharian, U. Sennhauser, B.J. Nelson: Batch fabrication of carbon nanotube bearings, Nanotechnology **18**, 075703 (2007)

18.214 P. Kim, C.M. Lieber: Nanotube nanotweezers, Science **286**, 2148–2150 (1999)

18.215 L.X. Dong, A. Subramanian, D. Hugentobler, B.J. Nelson, Y. Sun: Nano Encoders based on Vertical Arrays of Individual Carbon Nanotubes, Adv. Robot. **20**, 1281–1301 (2006)

18.216 I. Asimov: *Fantastic Voyage* (Bantam Books, New York 1966)

18.217 R.A. Freitas: *Nanomedicine, Volume I: Basic Capabilities* (Landes Bioscience, Austin 1999)